Defense Intelligence Reference Document

Defense Futures

01 November 2010

ICOD 30 August 2010

DIA-08-1011-001

Laser Lightcraft Nanosatellites

The **Defense Intelligence Reference Document** provides non-substantive but authoritative reference information related to intelligence topics or methodologies.

Prepared by:

(b)(3):10 USC 424

Defense Intelligence Agency

Author:

(b)(6)

Administrative Notes:

(U) COPYRIGHT WARNING: Further dissemination of the photographs in this publication is not authorized.

This product is one in a series of advanced technology reports produced in FY 2010 under the Defense Intelligence Agency, (b)(3):10 USC 424 Advanced Aerospace Weapon System Applications (AAWSA) Program. Comments or questions pertaining to this document should be addressed to (b)(3):10 USC 424;(b)(6) (b)(3):10 USC 424;(b)(6) AAWSA Program Manager, Defense Intelligence Agency, ATTN: (b)(3):10 USC 424 Bldg 6000, Washington, DC 20340-5100.

Contents

Figures

Tables

Laser Lightcraft Nanosatellites

Summary

Miniaturized satellites are spacecraft of unusually low mass and small size, usually under 500 kg in total mass. The term "minisatellite" refers to a spacecraft with a wet mass (including onboard propellant) of 100 kg to 500 kg. Microsatellite or "microsat" is a spacecraft with a wet mass of 10 kg to 100 kg. Nanosatellite or "nanosat" is a spacecraft with a wet mass below 10 kg. Picosatellite or "picosat" is a spacecraft with a wet mass of 0.1 kg to 1.0 kg. Picosats are also called sub-nanosats.

The primary reason for miniaturizing satellites is to reduce cost. Heavier satellites require larger launch vehicles of greater cost while smaller, lighter satellites require smaller and cheaper launch vehicles and can sometimes be launched in multiples or "piggyback" using excess capacity on larger launch vehicles. Miniaturized satellites allow for cheaper designs as well as ease of mass production. However, few satellites of any size other than communications constellations, where dozens of satellites are used to cover the globe, have been mass produced in practice.

Besides the cost issue, the main rationale for the use of miniaturized satellites is the opportunity to enable missions that a larger satellite cannot accomplish, such as:

- Constellations for low data rate communications.
- Using formations to gather data from multiple points.
- In-orbit inspection of larger satellites.

Many of these missions require numerous small spacecraft in a constellation or "swarm." These include orbital communications networks and swarms of small satellites to conduct remote sensing, and to provide unique perspectives on astronomical bodies of interest. For instance, 100 or more nanosats could be deployed from a mother ship to their final destination in space for deployment.

Provisions for orbital maneuvers as well as attitude control, multiple sensors, and instruments, and full autonomy will yield a highly capable miniaturized satellite. All onboard electronics will survive a total radiation dose rate of several hundred kilorads over a several year mission lifetime (at least 100 kilorads over two years). Nanosats developed for in-situ measurements will be spin-stabilized, and carry a complement of particles and fields instruments. Nanosats developed for remote sensing measurements (MASINT) or surveillance and eavesdropping (SIGINT) will be three-axis stabilized, and carry a complement of imaging and radio wave instruments. Autonomy both onboard the nanosats and at the ground stations will minimize the mission operational costs for tracking and managing a constellation.

To reduce overall mission cost, advanced technology components and a novel laser propulsion system will be used to make nanosats and their onboard instruments compact, lightweight, low power, low cost, and able to survive their radiation environment over a several year lifetime. Each nanosat will be manufactured and tested for a recurring cost not to exceed $500k. By producing a large quantity of nanosats for a given mission, the per-unit cost will be reduced to a small fraction of

1

satellite procurements for traditional missions. Mission operation costs will be minimized by the incorporation of both onboard and ground autonomy and use of heuristic systems.

2

Chapter 1: Nanosatellite Technologies

OVERVIEW

Nanosats require technologies that radically reduce the mass and power of components without compromising performance. In addition to miniaturizing components, methods to integrate similar functions across subsystems are being evaluated. For example, all subsystem electronics, including instruments, could be integrated within the Command and Data Handling (C&DH) subsystem. Multifunctional solutions also offer significant savings over traditional approaches. Technology investments are required to develop or adapt components to accommodate the expected radiation environment. Simple, effective methods of thermal control are essential to keep the nanosat operational during extreme temperature variations. Autonomy is a critical technology that impacts every subsystem. Constellations with tens to thousands of nanosats must be highly autonomous to be practical. The nanosat ground system must be kept inexpensive, simple, and made inter-operable with other missions.

PROPULSION

In the baseline mission, nanosat propulsion is needed for two distinct functions: 1) each nanosat must raise its orbit apogee to the appropriate radius, 2) and it must reorient the axis of the spinning nanosat from the velocity direction (within the orbit plane) to its science mission attitude (perpendicular to the ecliptic plane). These maneuvers present challenging velocity change (Δv) and attitude-control (ACS) requirements.

Requirements for the Δv Thruster:

- Total impulse: 3,000 to 7,000 N-sec.
- Thrust: 445 N maximum.
- Input power (during burn): < 1 watt.
- Specific impulse: 280 seconds.

Requirements for the ACS Thruster:

- Total impulse: ≤ 2.4 N-sec.
- Minimum impulse bit: 0.044 N-sec.
- Response time: < 0.005 sec.
- Pulse rate: 1 Hz.

It turns out that the Δv and ACS thrusters can have independent systems. We propose a new innovation whereby the nanosat launch vehicle propulsion system also serves double duty as the Δv thruster system, and this can be done without having to carry the propulsion energy source into orbit. This can only be achieved via laser propulsion in which the laser beam energy that is used to launch a nanosat into orbit is also used to provide Δv thrust in orbit. This novel innovation dramatically reduces the mass, size, cost, and complexity of nanosats because they will only need to carry minimal onboard ACS thrusters and propellant to carry out routine, minor attitude adjustments. The innovative nanosat laser propulsion concept is presented in Chapter 2.

Miniaturized solid propellant gas generators could be used as ACS thrusters. Forty-eight 50 mN-sec pulses are required to reorient the nanosat after it achieves the required orbital altitude. Although this could be achieved either by a monopropellant or a cold gas thruster, it could also be achieved using an array of gas generators. Such miniaturized gas generators have already been successfully built and commercialized by companies such as MOOG and Lockheed-Martin Space Systems. By incorporating micro-electromechanical systems (MEMS) techniques, the devices have been produced relatively inexpensively. Miniaturized electric propulsion ACS thrusters, such as pulsed plasma and MEMS field-emission electric propulsion (MEMS FEEP) thrusters, have been developed and are now emerging into widespread commercialization.

GUIDANCE, NAVIGATION AND CONTROL

Guidance Navigation and Control (GN&C) subsystem key technologies and concepts have been identified to enable successful altitude determination of spin-stabilized and three-axis-stabilized nanosats for future missions. They include miniaturization of a sun sensor and horizon crossing indicator. The miniature precision "fan" sun sensor will pinpoint the sun virtually everywhere in the entire celestial sphere with every satellite rotation. The sun sensor will be required to weigh less than 0.25 kg, draw less than 0.1 watt, operate on no greater than a 3.3 volt bus, and meet a $0.1°$ resolution requirement. The miniature horizon crossing indicator has a small bore-sight field of view that is mounted at an angle off the spin axis. As the spacecraft rotates, a cone of coverage is formed. The sensor must be capable of detecting Earth over a range of orbital radii with a pointing accuracy of $0.05°$. Total horizon crossing indicator weight and power will be less than 0.2 kg and 0.1 watt, respectively.

Of particular interest to Constellation missions is the incorporation of GPS onboard the nanosats, to eliminate ground-based ephemeris generation. This allows for increased autonomy and simpler, more accurate time resolution onboard the spacecraft. For GPS to fit within the constraints of a nanosat, the receiver electronics need to be miniaturized into a layer within the C&DH module.

COMMAND AND DATA HANDLING

Developing the C&DH subsystem for a nanosat presents some unique challenges, with low mass (0.25 kg) and low power (0.5 W) requirements being the biggest drivers. Advanced microelectronic solutions are being developed to meet these challenges. The microelectronics developed must be modular and of scalable packaging to both reduce cost and meet the requirements of various missions. This development will utilize the most cost effective approach, whether infusing commercially driven semiconductor devices into spacecraft applications or partnering with industry in the design and development of high capacity data processing devices. The major technologies will include: lightweight, low power electronics packaging; radiation hard, low power processing platforms; high capacity, low power memory systems; and radiation hard, reconfigurable, field programmable gate arrays (RHrFPGA).

The C&DH requirements are as follows:

- Power: 0.5 watts.

4

- Weight: 0.25 kg.
- Input data rate: 2 kbits/sec.
- Output data rate: 100 kbits/sec.
- Data storage: 2 Gbits.
- Encoding: advanced convolutional.
- Processing speed: 12 MIPS.
- Radiation tolerance: > 100 krads total dose.

In order to develop a low mass C&DH, a lightweight and low power electronics packaging method must be used. The packaging method that will be chosen must have a small volume and small footprint (6 cm × 6 cm × variable height). The packaging technique must provide data on programmable substrates and data on a compliant interconnects for space use. A multi-chip module (MCM) has been successfully produced by Pico Systems Inc.

A combined effort to reduce mass, power, size and cost led to the development of the CMOS Ultra Low Power Radiation Tolerant (CULPRiT) system on a chip, and "C&DH in your Palm" are technologies that enable the power reduction required for nanosats. The goals of these technologies are a 20:1 power reduction over current 5-volt technology, foundry independence of die production, and radiation tolerance.

Another technology enabling a decrease in volume is the RHrFPGA, which reduces volume by replacing many logic functions/circuits with one die. The RHrFPGA also allows concurrent design by decoupling the logic design from the module, shortens the design schedule, lowers the part count, and eases rework.

The above technologies allow for higher levels of electronic integration, effectively combining spacecraft subsystem electronics and instrument electronics into the smallest possible mass, power, and volume.

POWER SYSTEMS

Total spacecraft power is limited by the small satellite size. The Sun's power density is 1.35 kW/m^2. Assuming 15% conversion efficiency for a 0.3 m × 0.1 m disk shaped nanosat (cross section of 0.03 m^2), with a 67% area coverage, this results in a total electric power of only 4.0 watts. Lightweight, efficient solar array panels that minimize the effective array mounting area are needed. Dual or triple junction GaAs solar cells that give 18% conversion efficiency at end of life (EOL), and assuming a more optimistic area factor of 85%, will result in only 6.2 W at EOL. Small satellites that do not have extended solar panels simply do not intercept a large solar power density and must use the available power very efficiently. For a small spinning satellite, it is expected that three solar cells will be connected in series along the spin axis, and groups of three will be connected in parallel around the circumference. Each section will generate 3.3 volts and rotate into and out of sunlight as a unit. Voltage drops at 3.3 volts, bus regulation, circuit protection (e.g., fuse or circuit breaker) and Lithium ion battery discharge characteristics are being studied.

Highly elliptical orbits in the ecliptic plane where the apogee velocity is very low will cause a several hour eclipse during part of the year. Spacecraft batteries to cover this eclipse period presents a significant mass impact. However, only a 10° orbit plane

5

inclination relative to the ecliptic, will reduce the maximum eclipse period to about one hour. Inclusion of spacecraft batteries is then justified. Passive thermal control will be used to keep the spacecraft electronics within 10°C of ambient temperature, and hence will not require electric power for heating. Using such a scenario, a battery requirement of about 2 amp-hours at 3.3 volts will allow full spacecraft functionality during an eclipse. Twelve AA size Lithium-ion batteries meet the requirement and only weigh 480 grams.

Circuits that have high current demands, such as thruster solenoids and fuses, need to be augmented with components that have a lower power density than batteries, but also have lower internal resistance. Ultra-capacitors are being explored for this application.

Miniaturization of the power system electronics (PSE) to meet the weight and size requirements of the nanosats is a considerable challenge. The ideal approach is to eliminate the PSE completely, by having a fixed electrical load and batteries provide the needed bus regulation. This yields a simplified system consisting of solar cells, batteries, and minimal circuitry. A more immediate approach to miniaturization is to produce hybrid modules that measure approximately 5.08 cm × 3.17 cm × 1.27 cm and weigh 100 grams for each PSE component, namely the solar array regulator, battery regulator, and low voltage power converter. The combination of these three components into one module will reduce the size and weight another order of magnitude.

THERMAL

Although an inclination change by 10° renders maximum shadows below two hours, we evaluate the case of a maximum eight hour shadow for the purpose of generality. Three thermal configurations are considered: (1) top and bottom of the nanosat are insulated, the inside of the cylindrical solar array is not insulated, allowing internal heat transfer between the internal equipment and the array; (2) the entire nanosat is insulated, top and bottom as well as inside the solar arrays, except for a radiator on top, sized to radiate the internal electrical dissipation; and (3) the internal equipment is thermally isolated as well as possible from an "outside shell" with a controllable two-phase heat transport device which can be "shut off" during Earth shadows, serving as the only thermal coupling between the equipment and a radiator on the outside surface.

The key advantage of configuration (1) is its reliability, or robustness. Since the temperature of the nanosat is set by a high energy balance (heat in – heat out) dominated by the absorbed solar energy, the operational temperature of the nanosat is relatively insensitive to top and bottom multilayer insulation (MLI) properties, or, largely, to internal heat dissipation. However, the feature that yields the operational reliability, i.e., the high energy balance, also results in a rapid drop in temperature when the solar load disappears during the Earth shadow. During the maximum eight hour eclipse used for this evaluation, it was found that internal temperatures dropped by about 60°C, which would result in internal temperatures in the range of –30°C to –40°C. At the same time, the solar arrays dropped to a temperature of about 60°C. Based on past experience, these end-of-eclipse temperatures are reasonable.

Because configuration (2) has a much smaller overall energy balance than configuration (1), it is much more sensitive to MLI properties and to internal power dissipation. However, eclipse performance improves. During the ~ 8 hour eclipse, internal temperatures drop by only 20°C, a marked improvement, with end-of-eclipse temperatures well within the range of most spacecraft components. It should be noted that the solar arrays, since they are now isolated from the body of the nanosat, drop to temperatures of about –110°C. Even these solar array temperatures should not pose a problem. For example, the solar arrays of many geosynchronous satellites drop routinely to temperatures of about –150°C during the 72 minute eclipse experienced by these spacecraft at each equinox season.

The key feature of configuration (3) is that the equipment is coupled to an external radiator only with a two-phase heat transport device, such as a capillary pumped loop (CPL) or loop heat pipe (LHP). Operational temperatures are again maintained to temperatures of about 20°C nominal with a properly sized radiator. However, the temperature is also totally dependent on the proper operation of the two-phase "loop." The two-phase heat transport device can be made redundant by the addition of a second loop if single fault tolerance is desired. Note that redundancy is not a consideration for the other two configurations. During the ~ 8 hour eclipse, further improvement is realized, with internal temperatures dropping by as little as 6°C if the internal payload is well insulated from the exterior of the nanosat. As in configuration (2), the solar array temperatures drop to about –110°C. For certain equipment or science instruments, the temperature control afforded by this type of "active" design may be necessary.

A moderate amount of technology development has been underway since 2000 to enable a two-phase heat transport system for use in a nanosat. The small size and low heat transport requirements of the nanosat will necessitate significant downsizing of today's flight qualified two-phase systems. This reduction will be accomplished by leveraging recent successful tests of a small cryogenic two-phase CPL.

RF COMMUNICATIONS

The onboard RF subsystem must be small, low mass, and low power. The system specifications are:

- Mass: 0.5 kg.
- Power consumption: 0.5 watt.
- Transmission data rate: up to 100 kbits/sec.
- Command reception data rate: 1 kbit/sec.
- Range: 3 to 5 Earth radii.
- Channel type: BPSK.
- Effective isotropic radiated power: 0.15 watt (–8.2 dbW).
- Carrier frequency: 8,470 MHz.

The tracking system should be coupled with this communication subsystem to maximize efficiency in mass and power.

The communications subsystem is further complicated by constellations requiring spin-stabilized nanosats. A spinning nanosat cannot easily point an antenna toward Earth. Therefore, a low gain omni antenna is assumed and communications must take place near perigee, when the range is 3 to 5 Earth radii. A large ground antenna and high data rate compression must be used to achieve reasonable data rates with minimum power. This places an additional burden on the ground stations for both sensitive receivers/bit synchronizers and advanced decoders. These same considerations limit data rate for satellite-to-satellite communication.

Although the inclusion of an onboard command receiver is highly desired, it puts an additional strain on an already challenged nanosat mass and power budget. For this reason, the concept of a totally autonomous, receiverless nanosat design appears most attractive. However, "receiver-on-a-chip" technology has advanced to the point where including a receiver onboard looks feasible. The biggest disadvantage of a receiver now becomes the ground personnel and software needed to support the ability to command the nanosat. Command actions taken onboard will of course be limited to basic functions such as "transmit data" because of the lack of redundancy and mechanical functions. Although scenarios have been defined to allow nanosats to autonomously determine when to transmit their stored data, utilizing a receiver to control the telemetry downlink from the ground still has value. The capability of uploading flight software changes, as well as sending a master reset if necessary, would also exist with such an onboard command receiver.

MECHANICAL AND STRUCTURES

The nanosat mechanical system will be kept as simple as possible. The ideal nanosat mechanical design should consist of a one-piece structure on which all other components are mounted.

Multifunctional structures can provide thermal control, shielding and serve as substrates for printed circuit boards. For example, diamond facesheet honeycomb panels can serve as a structure, thermal conductor and radiator, and printed circuit board substrates. The diamond facesheet provides ten times greater thermal conductivity than aluminum and can dissipate heat from high power density electronics modules with a low mass comparable to carbon fiber composites. Another example is the structural battery system. It consists of a honeycomb panel whose core is filled with the cells of a nickel-hydrogen battery (or other flight qualified cell technology).

Concurrent engineering and fabrication techniques will be used to create a single computer model for the design, analysis (structural, thermal, and dynamic), and fabrication of the nanosat and its components. Dynamic modeling capabilities to simulate nanosat deployments will provide faster designs and a reduction in the amount of deployment testing required. This approach will significantly lower development costs by reducing duplication of effort, chances of errors, the number of drawings and paperwork required.

Mass production techniques not traditionally used for spaceflight hardware will be used, such as casting and injection molding. Options being considered for the nanosat structure material are: cast aluminum; cast aluminum-beryllium alloy; injection molded

8

plastic; fiber reinforced plastic; flat stock composite construction; and carbon nanotubes (a.k.a. "Buckytubes") or carbon nanotubes composited with other materials. The material will be selected based on mass, cost, manufacturability, ease of assembly and integration, and suitability for the space environment.

Streamlined testing is needed for up to 100 or 1000 nanosats per mission. Performing a complete test program on each unit would be prohibitively expensive and time consuming. We need to reduce the quantity of testing required while assuring product quality to meet program cost and schedule goals. Lot testing and statistical quality control methods should be developed to verify quality and structural performance by testing a small subset of the total number of nanosats.

INSTRUMENTS

Instruments for in-situ and remote measurements must be miniaturized to fit within the mass and volume constraints of a nanosat. Power consumption must also be scaled down accordingly. Instrument sensitivities cannot be compromised in the process. Instrument electronics need to be combined with nanosat subsystem electronics to achieve higher degrees of integration yielding reduced mass and volume. Instrument software will be designed to evaluate the onboard data and adjust instrument data rates and modes to efficiently capture the data of highest priority.

GROUND SYSTEMS

The large number of nanosats in a constellation is a challenge to the ground system in getting all of the data to the users. In a typical baseline mission, there are times when up to ten (or more) nanosats would be within communications range of a ground station at a single time. A minimal model for the ground station contacts shows that they can support a nanosat constellation with only two ground stations located on opposite sides of the Earth. The schedulers will prioritize the contacts, with the nanosats in the higher period orbits getting priority. Nanosats in the lower period orbits have more opportunities to dump their data, and therefore can have lower priority without risking any data loss.

Since the nanosats are autonomous, the operations concept for a mission requires only a few operators to determine the nanosat orbits, schedule the ground stations, and to investigate anomalies on the spacecraft. Automated systems will monitor the housekeeping data from the spacecraft and they will flag problems for the spacecraft engineers to investigate. The large number of nanosats allows the risk management to be different for this mission than for single spacecraft missions.

Except for commands to initiate the data downlink, the ground system will not command the nanosats for normal operations. The only commands that the ground system sends would be program loads to resolve or work around problems and failures.

The large number of nanosats in a constellation is a configuration control challenge for the data tracking, the schedules, the command loads, the science or intelligence data, and the engineering data. The ground system will use IDs, colorcoded user interfaces, and other techniques to ensure that the operators and users can keep track of the data

associated with a particular nanosat. Constellations that fly in close formation can benefit by the use of inter-nanosat communications to reduce ground station contention. The data would flow from a single nanosat to the ground instead of coming from every nanosat. Communications protocols for inter-nanosat communications must be developed.

AUTONOMY

Support costs are high if single-satellite mission operations and data analysis practices are scaled to a constellation mission. Autonomy onboard the spacecraft and on the ground is therefore required to ensure that mission objectives are efficiently and inexpensively met.

Nanosat autonomy will make use of onboard and ground-based remote agents with the overarching goal of maximizing the scientific or intelligence return from each nanosat during the mission lifetime. The remote agents achieve this goal by monitoring and appropriately controlling nanosat subsystems. Additionally, the onboard agent monitors the full complement of spacecraft sensors and instruments to heuristically separate scientific or intelligence events of interest from background events, thereby intelligently fitting the science/intelligence data within allocated spacecraft storage resources.

Nanosats with distant orbits are out of communications range of a ground station for nearly a week. Nanosat subsystems could be compromised if faults occurring during this blackout period were not readily addressed. An unacceptable loss of scientific or intelligence data could also occur. Therefore, the onboard agent will incorporate the capability to detect, diagnose, and recover from faults.

Certain failure scenarios may not be correctable by the onboard agent. These faults will be deferred to the ground agent for handling. Each nanosat will include data in its telemetry on the health and status of each subsystem and a history of commands autonomously issued since the last ground contact. The ground system will then attempt to diagnose problems based on this data. Additionally, collective knowledge of actions taken by all nanosats in the constellation will reside within the ground system by virtue of the data dumps made during each contact. From this data the agent can detect trends and systematic conditions not otherwise observable onboard the nanosat.

These highly autonomous systems will present a unique set of challenges not only to the system designers, but also to those involved in spacecraft testing. Careful consideration must be given to the design of the test program to ensure that the state-space of the remote agents is validated and verified. It is equally important to implement this program in a cost-effective manner. However, we could likely justify deploying considerable resources to address this issue since the methods developed to solve these challenges can be applied to numerous missions.

Chapter 2: Laser Lightcraft Nanosatellite Propulsion

Laser propulsion is a new and exceptional method for reaching space. By launching spacecraft on a beam of electromagnetic radiation, researchers will have developed the first new method of achieving orbit since the late 1950's. In this concept, a remote or ground-based energy source, such as a ground- or space-based laser beam generator, transmits power to a spacecraft via a beam of electromagnetic radiation [1-8]. The spacecraft collects the beam energy and uses it to power the propulsion system. This concept has the advantage of using the ambient air as the working fluid in the atmosphere and carrying propellant only for use outside the atmosphere, leaving the energy source for heating the propellant on the ground. This results in a tremendous weight reduction and improved performance benefit for the spacecraft because a large propellant mass and heavy energy source are not carried onboard.

The laser-propelled vehicle, called "Lightcraft" because it flies on a beam of laser light, is designed to harness the energy of a laser beam and convert it into propulsive thrust. In the earliest laser-propelled rocket designs, beamed energy from a ground-based laser (with near-visible wavelengths) is absorbed by a heat exchanger onboard a rocket, and is transferred to a working fluid. The heated fluid (hydrogen, ammonia, etc.) then produces thrust by expansion through a nozzle as in a conventional chemical rocket. An alternative to this scheme is to use the beamed-energy to ablate an onboard solid propellant (such as Delrin) to generate thrust. However, a more recent incarnation of this concept, developed by the Air Force Research Laboratory (AFRL) at Edwards AFB, CA, is for the Lightcraft to operate in two propulsion modes: airbreathing (detonation wave) and rocket ablation (deflagration). The Lightcraft operates in air breathing mode up to Mach 5 and 30 km altitude, and in laser thermal rocket mode (using liquid, gaseous, or Delrin ablation propellant) in space [7, 8, 9-16]. Figure 1 shows the Air Force X-25LR (25 cm diameter) Lightcraft concept. The Air Force X-50LR Lightcraft has twice the diameter as the X-25LR.
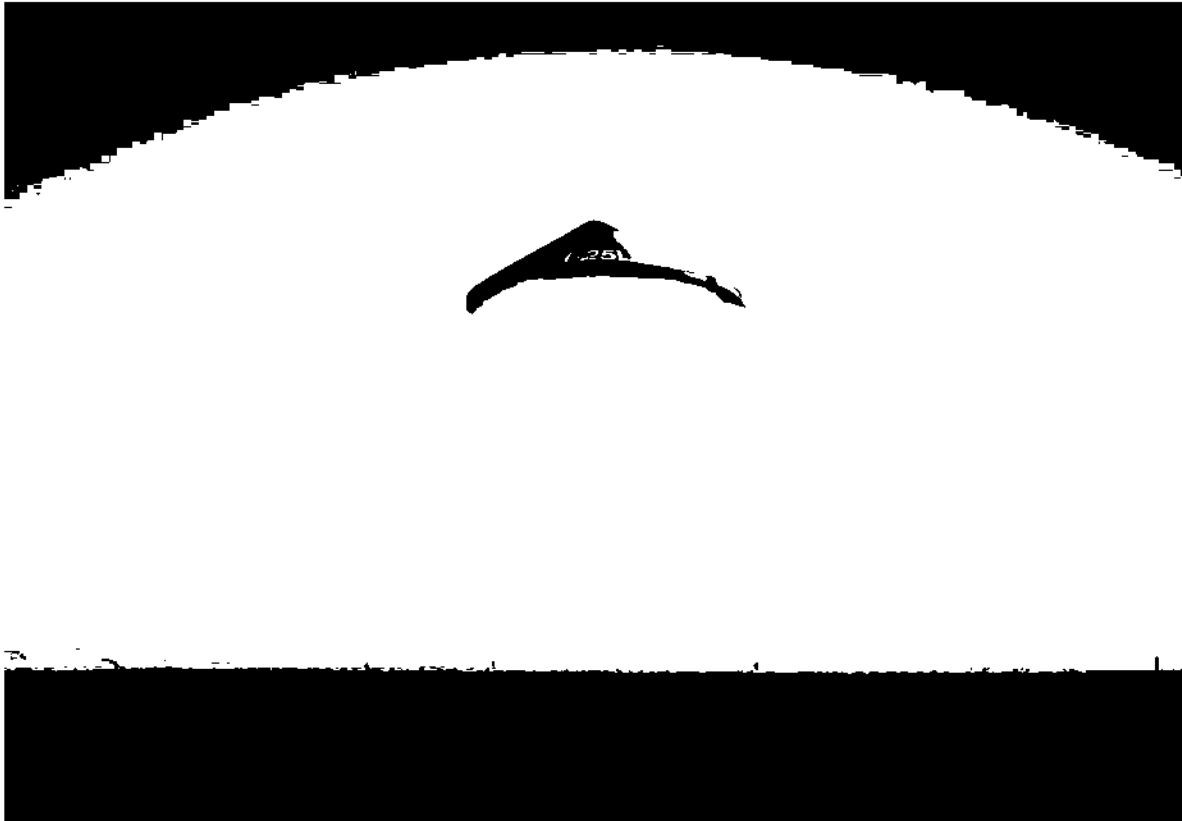
Figure 1. Air Force X-25LR Laser Lightcraft (courtesy of F. Mead, AFRL/PRSP, Edwards AFB, CA).

In the two-mode propulsion concept, a forebody aeroshell acts as an external compression surface for the airbreathing engine inlet. Affixed to the bottom of the craft is a parabolic-shaped afterbody mirror, which serves as a primary receptive optic for the laser beam and as an external plug nozzle expansion surface. The primary thrust structure is the centrally located annular shroud, which provides air through the inlet and also acts as a ring-shaped energy "absorption/propulsion" chamber for plasma formation. The air inlet is closed when the Lightcraft operates in the rocket mode.

The Lightcraft is very lightweight and uses its shape to facilitate vertical flight. The craft has the appearance of a fat acorn when viewed from the side. The lower portion of the craft is a very highly polished metal mirror, whereby the lower point of the acorn-shape is the midpoint of a stretched-out parabolic mirror (see Figure 2). The Lightcraft receives kilojoule pulses from a ground-based infrared laser at a rate of 25 times per second. The axisymmetric, off-axis parabolic collection mirror facilitates flight by concentrating the pulsed laser light into an annular focus. The laser beam's pulse interacts with the mirror, spreading out and focusing into an annular area inside the circumference of the craft. The intensity of the 18 microsecond pulsed laser is sufficiently high that atmospheric breakdown occurs in the annular area causing inlet air to momentarily burst into a highly luminous plasma (10,000 - 30,000 K), thereby producing a superheated plasma shock wave (with instantaneous pressures reaching tens of atmospheres) that generates thrust in the direction of the laser beam. A lip around the craft's circumference, akin to a plug nozzle, directs the expansion of the

plasma, creating downward thrust expansion. Multiple laser pulses and an atmospheric refresh of breakdown air generate the flight. This airbreathing pulsed-detonation engine concept owes its origins to the German V-1 "Buzz Bomb" of WW II which ran on aviation fuel.

For the purpose of this report, we envision a Lightcraft Earth-to-Orbit (ETO) transportation system that operates according to the following scenario. The airbreathing engine mode develops quasi-steady thrust by pulsing at a variable rate that depends on the Mach number and altitude flown along the flight trajectory to orbit. Once the Lightcraft reaches very high altitude and climbs above the atmosphere, it begins to operate in the thermal rocket mode using onboard propellant to convert and expand the laser energy for propulsion. The Lightcraft is spin-stabilized and can be launched vertically upward or on a slant upward trajectory, hover in mid-air, and undergo powered descent and landing. The ground-based laser beam generator system consists of the following: 1) power supply; 2) high-power (megawatt-class) laser beam generator/transmitter using novel beam optics; and 3) automated tracking, hand-off and safety systems.

HISTORY OF THE LIGHTCRAFT TECHNOLOGY DEMONSTRATION PROGRAM

The laser Lightcraft project originally grew out of the Lightcraft Technology Demonstration Program funded by the Strategic Defense Initiative Organization (SDID) Laser Propulsion Program in the late 1980's. In the 1990's, a joint program involving the NASA-Marshall Space Flight Center and the Propulsion Sciences and Advanced Concepts Division of the AFRL Propulsion Directorate developed and tested an experiment to determine the feasibility of using high-power pulsed lasers to launch a spacecraft into orbit. Successful tests at the White Sands Missile Range (WSMR) High Energy Laser Systems Test Facility (HELSTF) demonstrated the first passively controlled vertical free flight of an object that was propelled by the U.S. Army's 10 kW Pulsed Laser Vulnerability Test System (PLVTS) infrared CO_2 laser. Laser boost capability was demonstrated at the HELSTF with a Lightcraft reaching 43 m vertically in 2-second gyroscopically stabilized free flights, which was followed by horizontal guide-wire flights of 121.9 m lasting 10 to 20 seconds (see Figure 2 through Figure 6). A subsequent series of test flights achieved an altitude of 38.7 m. L. Myrabo (private communication, Rensselaer Polytechnic Inst., Troy, NY, 2009) recently reported vertical Lightcraft test flights achieving 68 m altitude.

This achievement can be compared to the first successful flights of Robert Goddard's liquid propellant chemical rocket, which attained a height of 12.5 m after a 2.5 second burn in March 1926. In sharp contrast with Goddard's rockets, there is absolutely no fuel on board the prototype Lightcraft, which has a diameter of 10 cm, mass of 20 to 40 g, and is machined from a solid block of 6061-T6 aluminum. Five different Lightcraft designs have been flight-tested using the pointing and tracking system on the PLVTS laser. Current Lightcraft designs are limited to about 60 g mass and 15 cm in diameter by the PLVTS laser. A megawatt-class laser will be necessary for a larger kilo-class Lightcraft to reach orbit and components for these lasers exist, which would demonstrate the feasibility of this technology for low cost access to space.
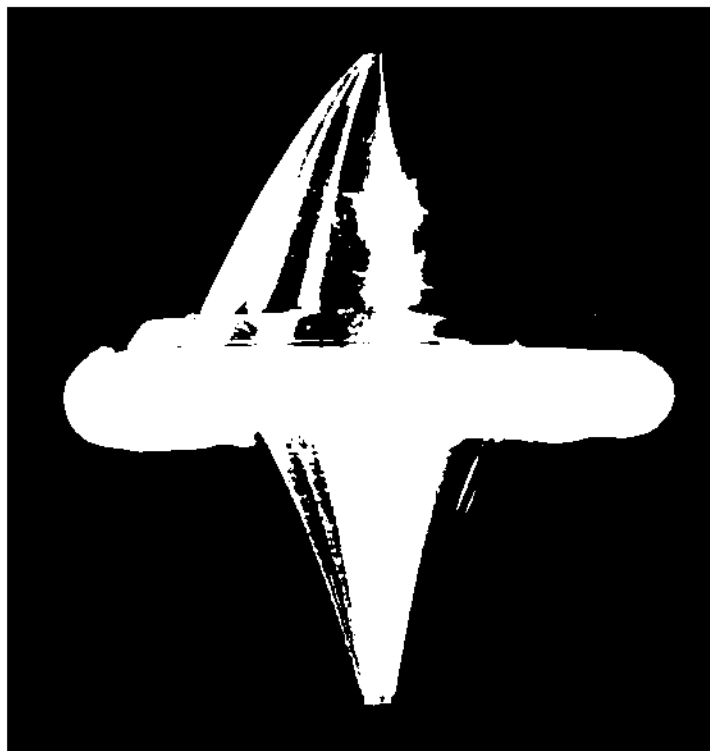
Figure 2. AFRL Test Vehicle in Vertical Flight (courtesy of F. Mead, AFRL/PRSP, Edwards AFB, CA).

14
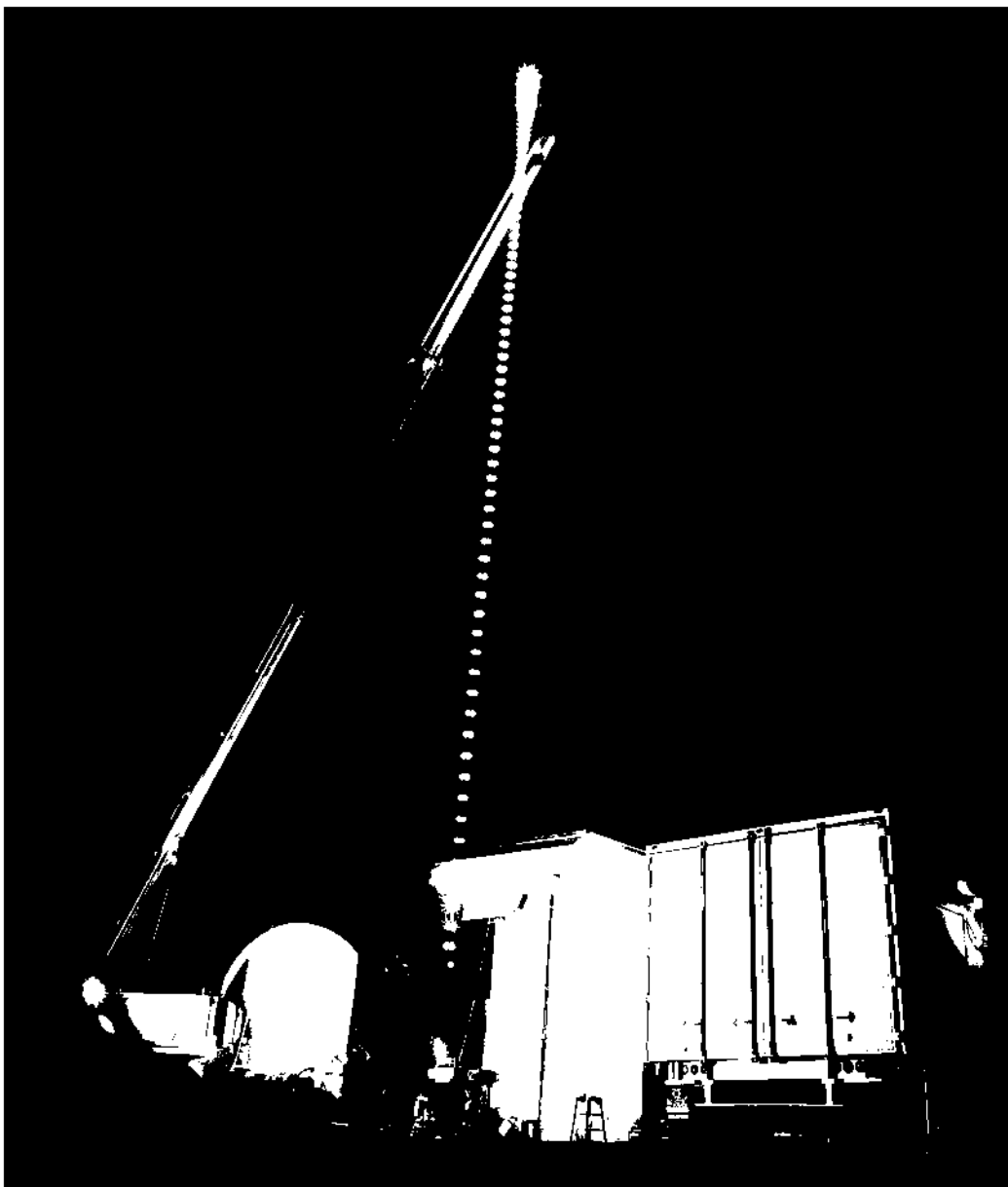
Figure 3. Time-Lapse Photo of a Lightcraft Undergoing an Outdoor Vertical Flight Test (courtesy of F. Mead, AFRL/PRSP, Edwards AFB, CA).

15

Figure 4. Lightcraft Flight-Test Vehicle Used in Horizontal Guide-Wire Flight Tests (the top of vehicle is to the right and the laser beam strikes the stretched-out parabolic mirror/propulsion section on the left) (courtesy of F. Mead, AFRL/PRSP, Edwards AFB, CA).

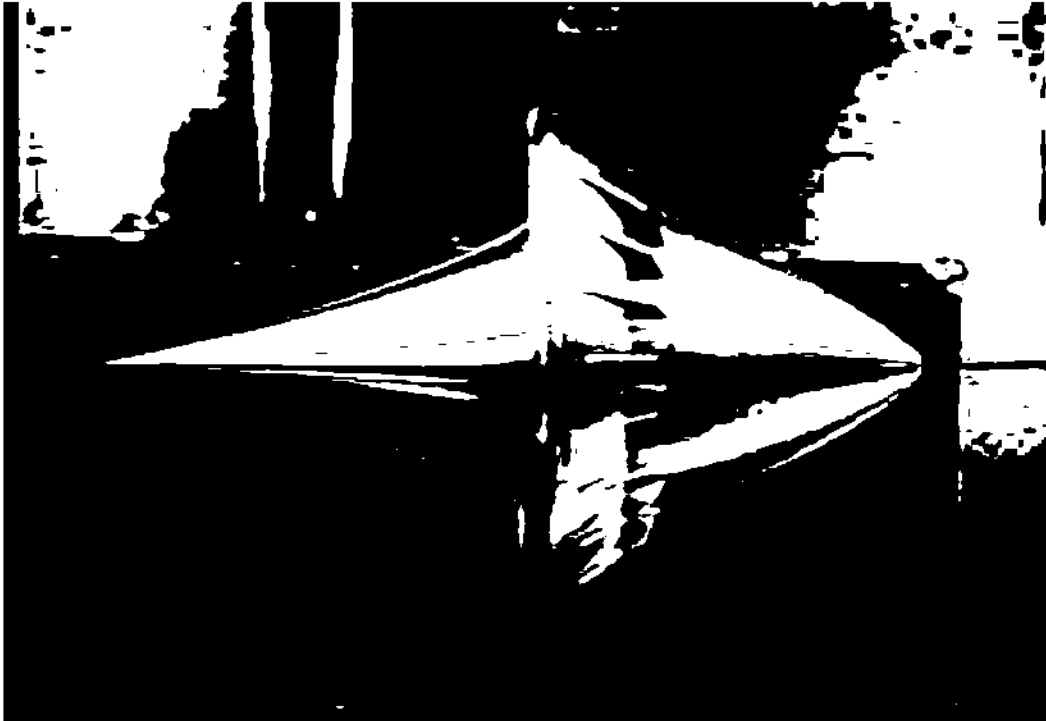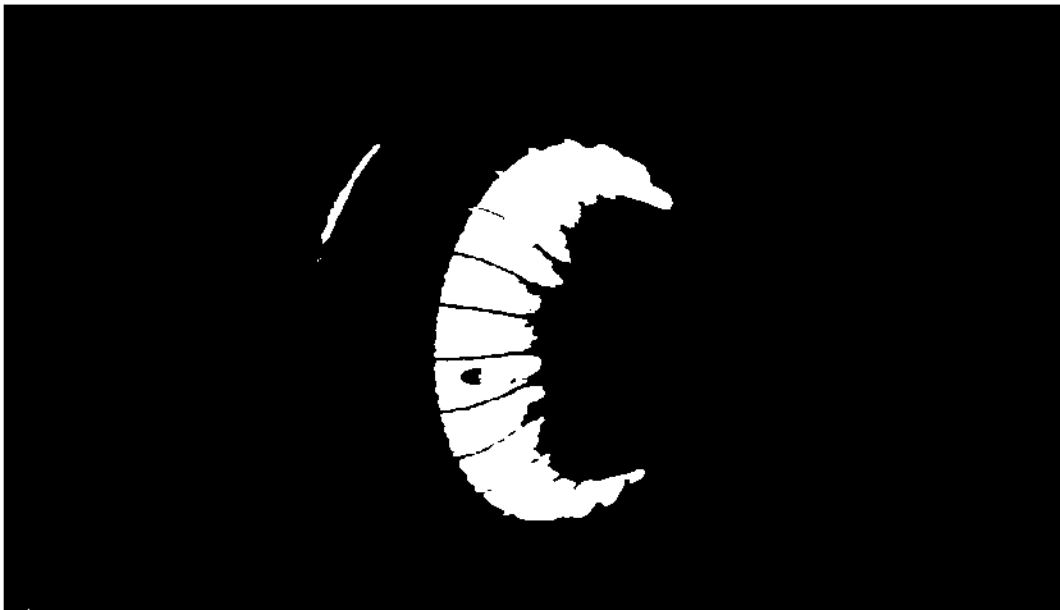Figure 5. Lightcraft Undergoing Horizontal Guide-Wire Flight Test (courtesy of F. Mead, AFRL/PRSP, Edwards AFB, CA).
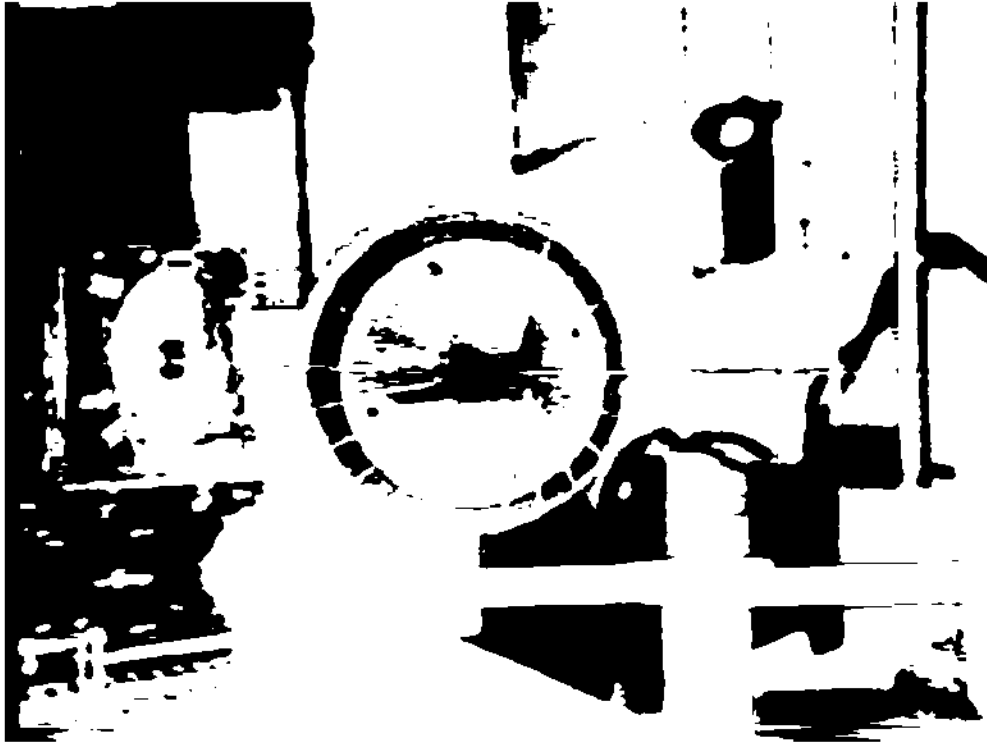
Figure 6. Lightcraft Undergoing Horizontal Guide-Wire Flight Test (courtesy of F. Mead, AFRL/PRSP, Edwards AFB, CA).

SUMMARY OF TECHNICAL PERFORMANCE AND BENEFITS

We outline below the propulsion performance features of the laser Lightcraft launch system:

- The system is single-stage-to-orbit and completely reusable.

- Almost no onboard propellant is required (the reaction mass is free air), except for the small internal amount of propellant needed for final ascent to orbit and orbital maneuvering.

- Vehicle specific impulse (I_{sp}) is essentially infinite ($\approx$ several $\times$ 10^3 seconds in rocket mode).

- Payload mass fractions are $\approx$ 50 - 95%.

- These systems are simple, reliable, safe, environmentally clean, and could have a very high all azimuth on-demand launch rate.

- Reduces space launch costs by two to three orders of magnitude below today's levels: estimated launch costs are $20/kg to $600/kg of payload (not including life cycle and launch operations costs).

- The feasibility and physics principles have been proven by the AFRL's Lightcraft Concept Demonstration Program [11, 16-25].

Lightcraft systems have sufficient power density to operate as ETD launch systems. It requires a beam power of 0.1 to 1 MW per kg of vehicle mass, while orbit-to-orbit

17

propulsion requires a modest 0.1 to 10 MW of total beam power. The ground-based megawatt-class laser beam generator is state-of-the-art technology. The cost of generating electrical power for the ground-based laser beam generator is ~ $0.10/kWh, which translates to < $2/kg of payload. An SDIO study [10, 11] showed that all launch to orbit conditions for a Lightcraft could be satisfied by a single, high-power ground-based laser – with or without the aid of a low altitude laser relay mirror or space-based laser beam generator system. The majority of the system mass required to launch a payload to orbit is left on the ground in the form of the beam generators and their electrical power sources. The dry spacecraft mass can be further reduced by two orders of magnitude, and thus the operating costs reduced by a factor of 10 (to < $2/kg of payload), if Buckytubes are used to construct the vehicle and its subsystems.

LIGHTCRAFT NANOSATELLITE CONFIGURATION

As shown in Figure 7, the Lightcraft nanosat configuration consists of: 1) a conically shaped "forebody" for lift and aerodynamic compression of ingested airflow (prior to its detonation by laser heating during atmospheric flight); 2) an annular "cowl" or "shroud" within which air detonation or propellant ablation (by intense laser heating) occurs; and 3) a parabola-shaped "afterbody" whose mirrored surface focuses beamed laser energy into regions of sufficient smallness for intense air or propellant heating to occur. And as shown in Figure 8, the vehicle is powered by laser airbreathing propulsion (by detonation of air) until hypersonic speed within the sensible atmosphere is reached; and then the vehicle is powered by laser rocket propulsion (by heating of propellant) during flight above the sensible atmosphere, until cut-off velocity for orbital flight is reached.

Shroud (Cowl):
within which Laser
Heating of Airflow
and Propellant
Occurs

• Laser Airbreathing Flight
from Zero Velocity to
Hypersonic Speed

Afterbody: with
Mirrored Surface
for Focusing Laser
Energy into the
Shroud (Cowl)

Laser
Beam

Forebody: for Lift
and Compression
of Airflow during
Atmospheric Flight

Axi-Symmetric Body

• Laser Rocket Flight from
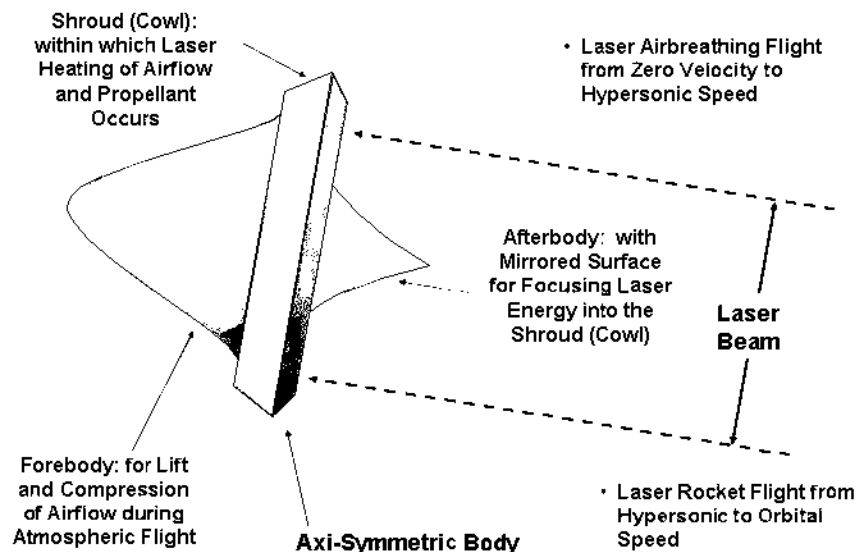Hypersonic to Orbital
Speed

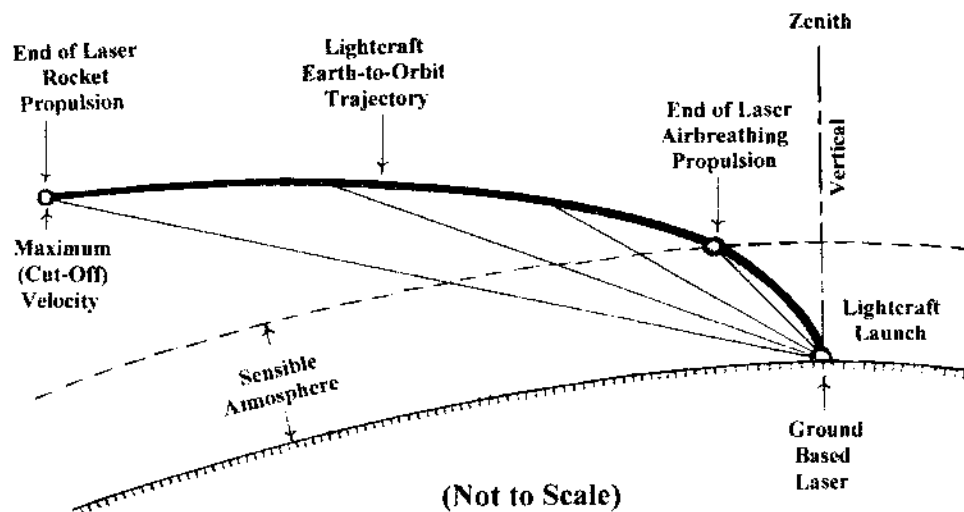**Figure 7. Lightcraft Concept** [26].

Figure 8. Lightcraft Trajectory and Associated Pointing Angles [26].

The low vehicle propellant fraction for laser powered Lightcraft ($\sim$ 0.5 of vehicle takeoff mass) resulted in vehicle takeoff masses that were approximately 45, 80, and 360 times less than those of conventional rockets for placing masses of 10 kg, 5.0 kg, and 1.0 kg into low Earth orbit (LEO). And preliminary life-cycle cost estimates made during the AFRL study by Froning and Davis [26] indicated that transportation system costs for placing 10 kg, 5.0 kg, and 1.0 kg of mass into orbit using Lightcraft and ground-based lasers would be approximately 3, 5, and 15 times less than with conventional rockets.

One of the two most important findings from the Froning and Davis study is the significant influence of Lightcraft drag on airbreathing laser propulsion performance, and the consequence of this on laser rocket propulsion performance during the latter phase of Lightcraft flight. As indicated in Figure 9, a significant reduction in both Lightcraft size and drag coefficient (C_D) – as compared to that of the initial government baseline design – was needed for acceptable airbreathing thrusting acceleration during atmospheric flight. Figure 9 shows that both size and drag coefficient reduction were accomplished in several steps – with both size and C_D reduction accomplished during the first step, and further C_D reduction (by increased forebody fineness ratio) during the second step.

It was also found that sufficient Lightcraft airbreathing thrust required thrust variation with altitude, somewhat comparable to that achievable by contemporary airbreathing propulsion systems – whose flight dynamic pressure (q) and thrust remain constant with increasing vehicle altitude and speed until constant q can no longer be maintained. Here, acceptable airbreathing thrust minus drag performance was needed to reach maximum airbreathing speed (Mach 10) within acceptably short flight times and distances. And such short times and distances were required to ensure adequate receipt of beamed power by the Lightcraft out to the longest ranges associated with laser rocket propulsion flight; where beamed power would travel the longest distances through the atmosphere and space, and collected power would drop to lowest values.

19

Froning and Davis [26] also determined that the ground-based laser selected (λ = 1.62 μm, 10 MW radiated power, 10 m diameter aperture) would enable a Lightcraft takeoff mass of 8 kg and Lightcraft propellant mass of 4 kg. Therefore, this would allow approximately 4 kg of mass to be placed into orbit with the selected ground-based laser. And vehicle synthesis work determined that the remaining masses for the Lightcraft airframe, propulsion, and control systems would be 0.63 kg, 0.46 kg, and 0.45 kg, respectively, together with a 30 percent contingency (of 0.47 kg).
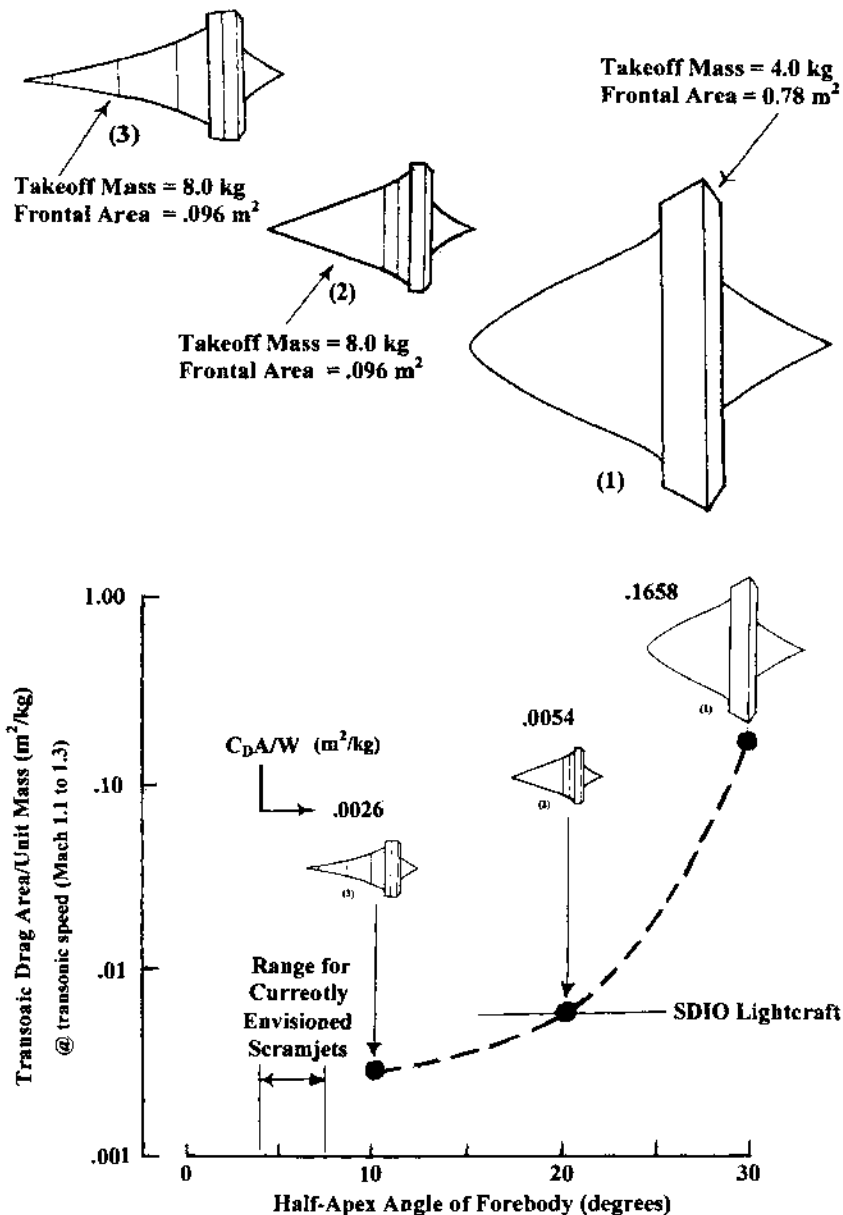

Figure 9. Lightcraft Vehicle Evolution (in 3 steps) [26].

Froning and Davis [26] further indicated that small COTS chemical propulsion systems, with sufficient thrust, would be about a factor of 7 to 12 heavier than those needed to meet Lightcraft orbit circularization needs. However, such mass reductions were

20

deemed possible with emerging MEMS technologies being developed under the National Nanotechnology Initiative for both chemical and FEEP thrusters (see Chapter 2 for details). It was also found that the currently configured composite structure for the Lightcraft forebody must be reduced from 2-ply to 3-ply (with the same ply-thickness) to meet Lightcraft airframe mass requirements.

Another important finding in the study was the significant influence of the ground-based laser wavelength (λ) on Lightcraft performance. Figure 8 illustrates the adverse beam propagation geometry associated with ETO laser propulsion by means of ground-based lasers. It is seen that beam propagation distances through the Earth's atmosphere are short during initial flight phases when the path length traveled by laser energy to the Lightcraft is least. But during latter flight phases (when the vehicle itself is above the sensible atmosphere) the beam propagation path within the atmosphere is much longer, and power losses due to atmospheric attenuation become ever greater with increasing range. And since power losses due to laser beam spreading – even in vacuo – also increase with increasing distance from the laser, power losses are greatest at the end of laser propulsion (when vehicle distance from the laser is greatest).

For a ground-based laser with given aperture diameter, adaptive optics, atmospheric conditions, and radiated power, the laser power collected by the Lightcraft was found to be extremely sensitive to laser wavelength. Here, λ determined the amount of radiated laser power lost through "thermal blooming," turbulence, and "extinction" during beam passage through the Earth's atmosphere in addition to the power lost from "diffraction" (beam spreading at longer ranges) during propagation through the vacuum of space. And since each loss mechanism was a function of λ, Froning and Davis considered each loss mechanism in their estimation of lost power for the six different laser wavelengths associated with the six different ground-based laser candidates that were evaluated in the study.

Shown in Figure 10 (without dimensions) is the fraction of radiated laser power collected by the Lightcraft at maximum laser propulsion range (when necessary "cut-off" velocity for orbital flight is achieved) for the spectrum of wavelengths investigated. It is seen that a significant fraction of laser-radiated power is lost, even if there were no atmospheric transmission losses at all. And additional losses associated with beam propagation through the atmosphere are seen to result in power losses on the order of 75% to 99%. Figure 11 shows that significantly more power would be available at the end of laser airbreathing flight than at the end of laser rocket flight. This might benefit surface-to-air Lightcraft missions that would mainly entail airbreathing flight.
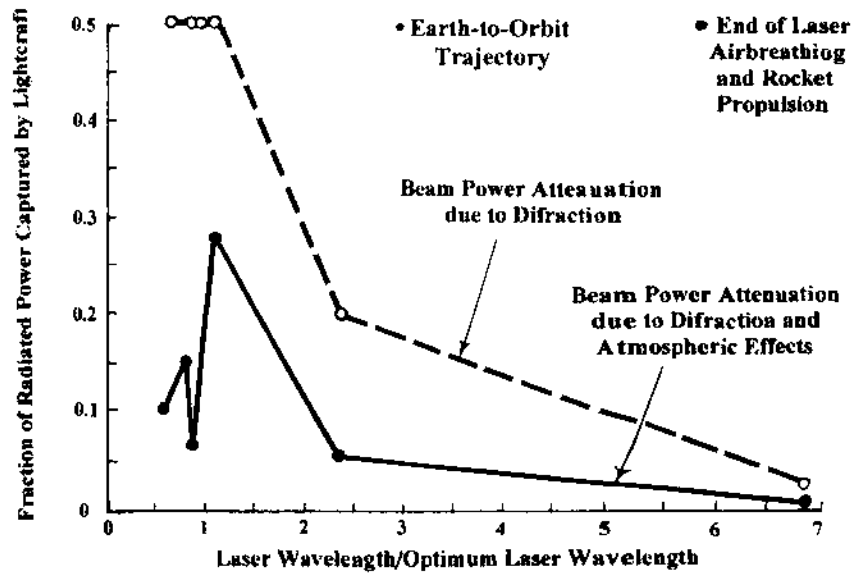
21

Figure 10. Attenuation Effects on Captured Laser Beam Power [26].
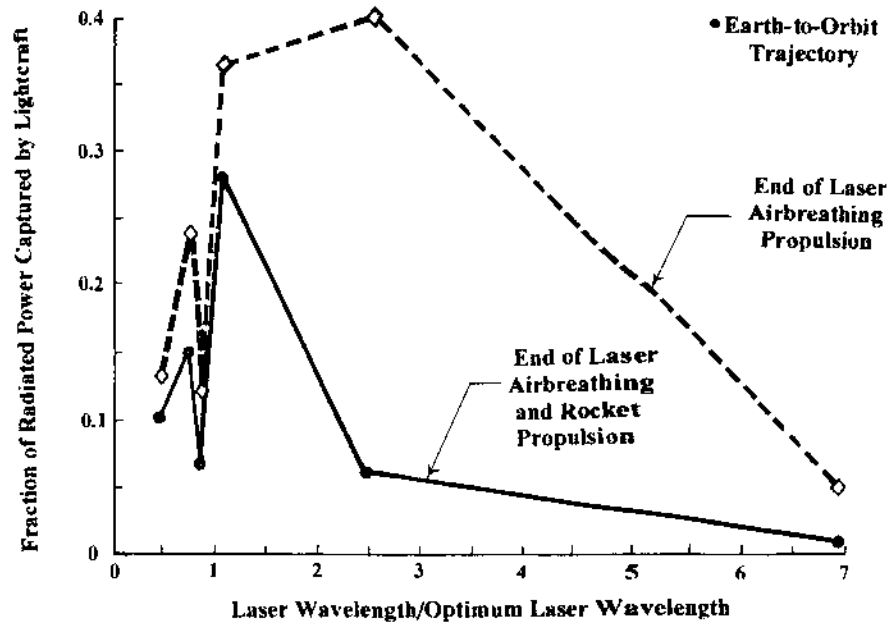
Figure 11. Influence of Trajectory and Laser Wavelength on Captured Power [26].

Figure 12 shows, for a given laser aperture diameter, adaptive optics, and atmospheric conditions, the decrease in laser power collected by the Lightcraft with increasing range from a 11.2 μm wavelength CO_2 laser. The decrease is shown for a vertical laser-pointing angle and for a final laser-pointing angle of 83° (from the vertical) that occurs at maximum laser propulsion range (about 500 km), where the Lightcraft reaches maximum speed.
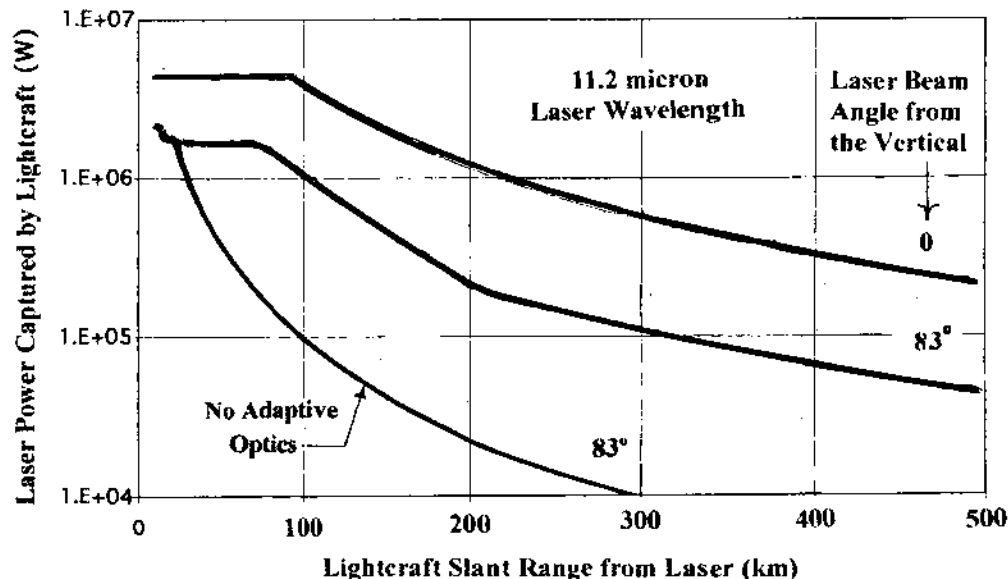
Figure 12. Captured Laser Power vs. Increasing Range from 11.2 μm CO_2 Laser [26].

Figure 13 shows the significant difference in the laser power collected by the Lightcraft during its laser propulsion phase of flight for the selected laser wavelength of 1.62 μm, and for the 11.2 μm CO_2 laser wavelength chosen for a government baseline Lightcraft. This comparison is for a Lightcraft trajectory determined from optimization work during the latter phases of the Froning and Davis study. It was also for the highest radiated power (10 MW) and the largest laser aperture (10 m) that was deemed practical for Air Force operations and systems.

Unfortunately the demonstrated laser beam power levels for the attractive 1.62 μm wavelength, which suffered the least propagation losses, are relatively modest. This attractive laser wavelength is associated with the wavelength-tunable free-electron laser (FEL), whose maximum beam power is currently in the 20 kW range. Thus, there is the need for a 500-fold increase in FEL beam power to achieve the 10 MW beam power required for (10 kg-class) Lightcraft ETO propulsion. However, 100 kW beam FEL designs are being proposed by the Navy for prototyping and testing in FY 2011 and 2012.

23
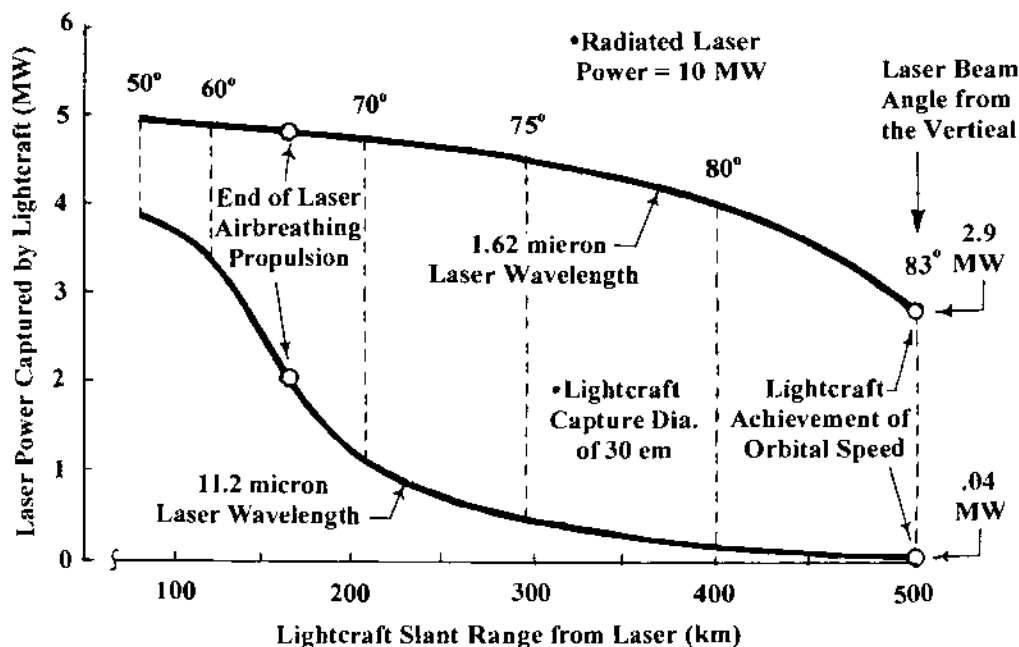
Figure 13. Influence of Lightcraft Range and Pointing Angles on Captured Power [26].

The physics and technology of FELs will allow beam power to be scaled up to 1 MW or higher as long as thermal loading of the beam optics and electron losses in the electron beam recirculation loop can be mitigated using engineering solutions. Beam combining of several 1 MW (or higher) FELs can achieve a total combined beam output power of 10 MW (or higher). Other newly emerging high-power laser technology that show promise for achieving megawatt-class beam power include bulk slab solid-state and high-power fiber lasers; the former has already achieved over 100 kW of beam power while the latter is getting close to it. Present megawatt-class lasers that are based on available proven technology include a proposal for a 5-beam, 2.5 MW per beam, electron gun-driven CO_2/gas mixture laser which combines five laser beams to achieve 10 MW of total beam output power. These systems will be described further in Chapter 4.

LIFE CYCLE OF LIGHTCRAFT SYSTEM

Froning and Davis [26] found that ground-based laser costs comprised the major portion of a Lightcraft ETO transportation system – with ground-based laser costs comprising about 80% of the total laser Lightcraft system life-cycle cost (LCC). The LCC of a laser Lightcraft ETO transportation system was estimated using Lightcraft vehicle and ground-based laser cost inputs from AFRL/PRSP together with programmatic cost inputs from another cost database. Table 1 shows the programmatic assumptions together with the system acquisition and operation costs for the various Lightcraft vehicle and ground-based laser system elements. Laser acquisition and operation costs were assumed to be shared with another user and all operations costs are reduced to one-half those values estimated from historical data. Launch costs are seen to be extremely low (only $74,141 per flight) with laser-

24

associated costs comprising approximately 92% of the laser-powered Lightcraft ETO transportation system LCC.

Table 1. Laser Lightcraft Model Cost Summary [26].

Laser Lightcraft Model Cost Summary	Share Solid-State Laser Cut Ops Costs by 50%	
Mission Model Length (Years)	10	
Launch Rate Per Year	1,000	
Payload Per Launch (kg)	2.0	
Mission Flight Time (s)	221.52	
Total Program Cost ($M)	741.410	
DDT & E / Acquisition Costs ($M)	680.358	91.77%
Operations Costs ($M)	61.053	8.23%
Average Cost Per Flight ($)	74,141	
Average Cost Per kg (based on operations costs) ($)	3,052	
DDT & E / Acquisition Costs ($M)	680.358	
Laser Lightcraft (LCC) Development Cost ($M)	18.000	2.65%
Laser Lightcraft (LCC) Acquisition ($M)	37.596	5.53%
10 MW Ground-Based Laser Acquisition ($M)	624.762	91.83%
Launch Site Facility Costs (Construction) ($M)	5.000	0.73%
Operations Costs, Annual ($M)	6.105	
Laser Annual Operations Cost ($M)	3.750	61.42%
Laser Refurbishment, Annual ($M)	0.750	12.28%
Laser Consumables, Annual ($M)	-	0.00%
Energy Cost, Annual ($M)	0.101	1.65%
Launch Site Facility Cost, Annual ($M)	0.250	4.09%
USAF Sys Prgrm Office (SPO) Cost, Annual ($M)	0.250	4.09%
NORAAD Coordination Cost, Annual ($M)	0.500	8.19%
FAA Coordination Cost, Annual ($M)	0.250	4.09%
Range (Safety, Tracking, Telemetry), Annual ($M)	0.255	4.17%

Chapter 3: Laser Lightcraft Weapon Mission Selection Study

The objective of the Froning and Davis [26] study was to examine crucial future Air Force launch vehicle missions and select at least one that might be performed very cost-effectively by Lightcraft vehicles powered by beamed electromagnetic energy from airborne or ground/sea-based lasers. It entailed identification and analysis of promising launch vehicle missions for laser-propelled Lightcraft, and assessments of the identified and analyzed missions by experts in the mission areas. See Figure 14 and Figure 15 for Lightcraft missions that have been identified and explored.

It was concluded that the most promising Air Force mission for a laser-propelled Lightcraft is the placement of Earth and space observing nanosats of up to 3 kg mass into LEO. Such a laser-propelled Lightcraft would also serve as a "Lightsat," because it would use the Lightcraft's laser propulsion optics as a telescope for observing military targets on Earth and in space. Additional estimated mass for performing the Lightsat function is no more than about 1 kg, if the Lightcraft forebody structure panels can be unfurled in orbit and used as solar power collectors. Such a Lightcraft system appears capable of reaching LEO at $1/5^{th}$ to $1/10^{th}$ the cost required for placing a similar Lightsat system into LEO using multistage chemical rocket systems.

Ground-to-Space

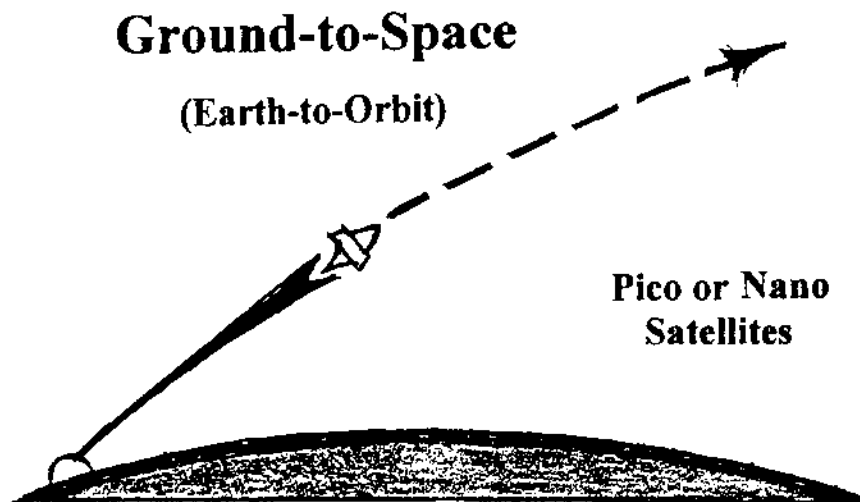**(Earth-to-Orbit)**

Pico or Nano Satellites

Figure 14. Ground/Sea-to-Space Concept: Appropriate rotation of a high-energy laser beam, emanating from a ground/sea-based laser, guides and propels an integral Lightcraft pico-/nano-satellite along an ETO ascent path until orbital conditions are reached, or until beamed laser energy can no longer be transformed into Lightcraft thrust [26].

Air-to-Space

(Ballistic Threats)

Enemy /
Ballistic Missiles

— **Air Launch:**
H ~ 12 km
V ~ M 0.8
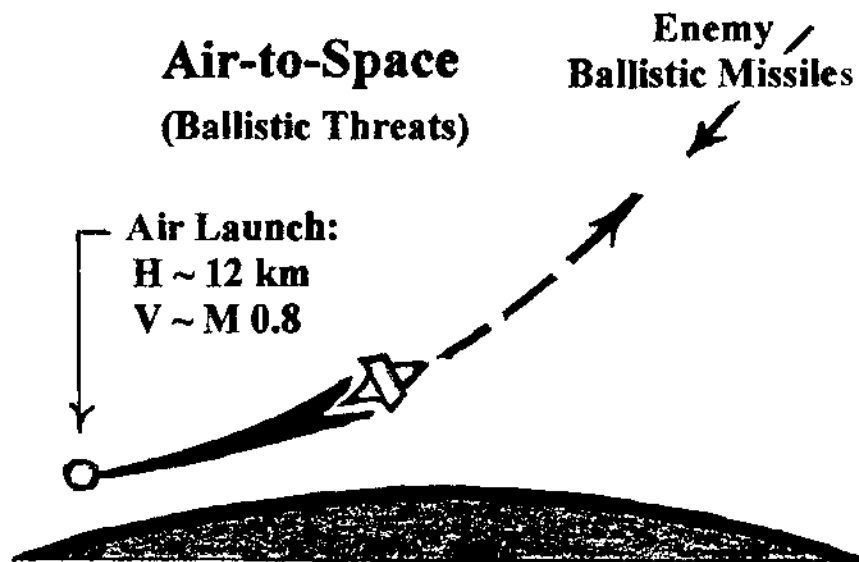
Figure 15. Air-to-Space Concept: Appropriate rotation and translation of a high-energy laser beam, emanating from a moving aircraft, guides and propels a Lightcraft toward a nearly head-on collision with an incoming ballistic missile; intermittently, the laser illuminates the target for guidance updates and for terminal semi-active seeker homing and end-game maneuvering [26].

ASSUMED LASER AND LIGHTCRAFT LIMITATIONS

Beamed power levels achievable with envisioned high-energy laser technology are assumed to be no more than about 10 MW for ground/sea-based lasers, and no more than about 2.0 MW for the much lighter and smaller airborne lasers installable on Boeing 747, B-1 Lancer, or C-130 subsonic aircraft. Lightcraft takeoff masses no more than about 20 kg can be accelerated to orbital velocities by maximum ground/sea-based laser power levels, and Lightcraft takeoff masses no more than about 4 kg to 8 kg, depending on the magnitude of velocity and acceleration needed, can be accelerated to very high velocities by the lower allowable masses and power levels of airborne lasers.

LIGHTCRAFT TRAJECTORY AND MISSION LIMITATIONS

Identified trajectory and mission limitations [26] are:

- Small allowable angle between centerlines of the laser beam and Lightcraft vehicle axes before significant thrust reduction occurs.
- Small allowable angles-of-attack (angle between Lightcraft centerline and velocity vector) before significant thrust reduction occurs.
- Limited capability for engaging multiple missile or aircraft threats in allowable time interval because of relatively long laser beam-riding time against each threat.

Additional Lightcraft hardware needed for some tactical missions [26] include:

28

- Terminal seeker guidance for hit-to-kill accuracy against missiles and maneuvering aircraft.
- Axial-/lateral-propulsion and control for missile and maneuvering aircraft interception.
- Additional mass along Lightcraft centerline for hardened target penetration.

LIGHTCRAFT MISSION INVESTIGATIONS: SUMMARY AND CONCLUSIONS

Ground/Sea to Space (ETO) [26]

If laser propulsion can provide nearly all Lightcraft Δv needed to reach LEO, then Lightcraft nanosat systems, which combine both launch vehicle and nanosat subsystems within a single vehicle, may be achievable with launch masses in the 2 kg to 10 kg range; and such Lightcraft nanosat systems appear capable of reaching LEO at 1/5th to 1/10th the cost required using multistage chemical rocket systems.

Air to Space (Air to Orbit) [26]

If hypersonic magnetohydrodynamic (MHD) airbreathing propulsion research and development currently underway at the NSF, NASA and the AFRL (Dayton, OH) is successful, then Lightcraft dry masses as heavy as 100 kg can be launched from aircraft flying at Mach 10 to 12 at about 30 km above the Earth. Such Lightcraft could be propelled by laser power as high as 100 MW that can be generated from the electrical power of ionized-air-slowing by interacting electric and magnetic fields within hypersonic MHD airbreathing engines.

Air to Space (Ballistic Missile Interception) [26]

Sufficient impact energy for destruction of high-speed ballistic missiles above the atmosphere is possible with chemical propulsion and uncooled IR detectors (for semi-active homing and axial/lateral acceleration during end-game) integrated into Lightcraft vehicles for an approximate 100% dry mass increase (from 1.0 kg to 2.0 kg). But multiple target interception within allowable time is limited by relatively long beam-riding time needed for the Lightcraft to reach and destroy each target.

Although laser-propelled Lightcraft appear capable of performing certain Air Force tactical missions, and are much less expensive than missiles currently used for such missions, the laser and aircraft costs associated with Lightcraft launches are much greater. Also, clouds impair Lightcraft air-to-ground and air-to-air effectiveness while air-to-air and air-to-space effectiveness is limited by long Lightcraft beam-riding times. Thus, no truly attractive Lightcraft combat mission was found. On the other hand, Lightcraft were found to be extremely attractive, compared to chemical rockets, in boosting microsats, nanosats, and picosats to LEO whereby the Lightcraft plus ground/sea-based laser costs are significantly less than multistage chemical rocket costs. Thus, the selected Lightcraft missions are launch vehicle missions involving

29

ground, sea and air launches of Lightcraft to LEO with air launch occurring at either subsonic or hypersonic speed.

Lightcraft Ground/Sea to Space Investigation

The current Air Force Lightcraft vehicle concept has been designed for not only placing nanosats into LEO at low cost (Figure 14), but also for performing much of the nanosat function as well. In this concept the precision optics system that focuses ground/sea-based laser light into the Lightcraft's cowl area for propulsion is also used as a space telescope for viewing military targets on Earth and in space. And structural panels on the Lightcraft forebody are also used as solar panels that are unfurled in orbit for generation of satellite power. Thus, the current Lightcraft's design allocates only 0.1 kg of its 1.0 kg dry mass for exclusively nanosat functions. There is a military need for 1.0 kg to 2.0 kg nanosats with optical sensors for visual inspection of unknown objects in space and on Earth.

Since conventional expendable rockets could conceivably be an alternative to laser-powered Lightcraft for the rapid placement of military nanosats in LEO, a cursory comparison of Lightcraft and conventional rockets was made by Froning and Davis [26] to get some idea of their comparative costs. Hybrid rocket sizing and costing was based upon tactical strategic missile sizing and costing information possessed by H. D. Froning. This information related costs (in 1982 dollars) to rocket and payload characteristics. Lightcraft sizing assumed a propellant mass fraction of 0.5 and 1.0 MW of laser power per pound of payload (dry mass) placed into orbit. Costs for laser power and refurbishment were based upon AFRL estimates (amortized over a fewer number of flights). Although these Lightcraft and laser costs are higher (based upon much fewer flights) than those of previous AFRL estimates, they are believed to be consistent with the conventional rocket costs, and therefore applicable for relative cost comparisons. More detailed future Lightcraft/conventional rocket designs and cost comparisons are, of course, needed before a strong argument can be made for either design.

Shown in Table 2 is the estimated performance and weights (masses) for 3-stage hybrid rocket launch vehicles and single-stage laser-powered launch vehicles that are capable of placing nanosats of 1.0 kg, 5.0 kg, and 10 kg into LEO. And Table 3 shows estimated costs for hybrid rockets and laser-powered Lightcraft assuming 100 flights over a 10-year period. These estimated costs indicate that Lightcraft could boost nanosats in the 2.0 kg to 5.0 kg range into LEO at about 1/10th to 1/5th the cost of expendable rockets. But Lightcraft cost superiority over conventional rockets is less overwhelming for satellites that are significantly heavier. Thus Lightcraft appear extremely attractive for satellite delivery missions only if Lightcraft dry masses, including the satellites being carried, are less than about 5.0 kg.

Table 2. Performance and Estimated Weights for a Hybrid Rocket and Lightcraft [26].

Hybrid Rocket Expendible Launch Vehicle – Assumed Performance and Estimated Weights			
Payload Mass (kg)	1.00	5.00	10.0
3rd Stage Wt. (kg)	36.8	71.2	108
3rd Stage Isp (s)	295	295	295
Propellant Fraction	.737	.766	.782
Impulsive Veloeity (km/s)	3.62	3.62	3.62
2nd Stage Wt. (kg)	283	311	341
2nd Stage Isp (s)	300	300	300
Propellant Fraetion	.800	.814	.830
Impulsive Velocity (km/s)	3.58	3.58	3.58
1st Stage Wt. (kg)	394	427	462
1st Stage Isp (s)	305	305	305
Propellant Fraction	.860	.868	.891
Impulsive Velocity (km/s)	1.92	1.92	1.92
Total Velocity (km/s)	9.12	9.12	9.12
Total Weight (kg)	715	815	921

Lightcraft Expeodable Lauoch Vehicle—Assumed Performance and Estimated Weights			
Payload Mass (kg)	1.00	5.00	10.0
Stage Wt (kg)	2.00	10.0	20.0
Effective Isp (s)	1,452	1,452	1,452
Propellant Fraction	.500	.500	.500
Impusive Velocity (km/s)	9.84	9.84	9.84

Table 3. Estimated Costs for Hybrid Rocket and Lightcraft Launch Vehicles for ETO Flight [26].

100 Flights

3-Stage Hybrid Rocket Launch Vehicle	1.0 kg Payload	5.0 kg Payload	10 kg Payload
Payload ($)	24,948	124,740	250,128
Boosters ($)	399,503	440,927	477,131
Integration ($)	96,163	101,441	123,941
Total ($)	520,615	667,108	851,200

Lightcraft Vehicle+ Ground Based Laser	1.0 kg Payload	5.0 kg Payload	10 kg Payload
Lightcraft ($)	24,948	124,740	250,128
Lightcraft Fuel ($)	2,495	12,474	25,013
Laser Power ($)	500	2,500	5,000
Laser Refurb. ($)	3,000	3,000	3,000
Total ($)	30,943	142,714	283,141

Rocketcraft Cost / Lightcraft Cost	16.82	4.67	3.00

1982 dollars multiplied by 1.62
(2.7% annual inflation) for 2000 dollars

Lightcraft Air to Space Investigation

One Ballistic Missile Defense (BMD) mission already being investigated by the Air Force for high-power airborne laser systems is the focusing of their intense beam energy on enemy ballistic missiles over dwell times sufficient to heat missile materials to high temperature thus causing structural failure. Another BMD mission that involves high-power airborne laser systems was examined during this investigation (see Figure 15). This mission entails ballistic missile destruction above the atmosphere during the missile's unpowered descent phase of flight. In this case, it is envisioned that the high-pulsed power within high-energy laser beams would first be used to rapidly examine each object within the incoming threat cloud and, based on each threat-object's response, discriminate warhead-carrying vehicles from lighter decoys and non-threatening debris. Next the pulsed power within the high-energy laser beam would guide a Lightcraft to the warhead-carrying vehicles while accelerating the Lightcraft to the flight velocity needed for warhead vehicle destruction by kinetic energy kill. And intermittently during the trajectory, the laser illuminates the warhead vehicle instead of the Lightcraft for guidance updates and terminal semi-active seeker homing.

Threats from space, other than ballistic missiles, were mentioned in the Rumsfeld 2001 Space Commission Report [27]. Dne threat to U.S. space assets specifically cited was microwave signal-jamming from relatively unsophisticated and inexpensive enemy satellites [28]. Eliminating such satellite threats has not been examined in detail, but they could be rapidly eliminated by air-to-space Lightcraft, if sufficiently precise azimuth and elevation information can be obtained to point Lightcraft lasers at the jammers.

"Hit-to-kill" accuracy and high impact energy requires Lightcraft maneuvering such that ballistic missile intercept occurs at relatively small angles from a head-on collision course. Tables 4 and 5 show the influence of such angles, together with Lightcraft velocity and enemy ballistic missile velocity, on Lightcraft impact energy and required mass. It is seen in both tables that intercept angles up to 45° from head-on collision courses do not significantly influence Lightcraft impact energy or required mass; that high Lightcraft impact energies are achieved with relatively low masses (1.0 kg); and that required Lightcraft masses for relatively high impact energies (10 MJ) are very low for Lightcraft velocities in the 2 km/sec to 4 km/sec range. It is also seen that the interception of longer range ballistic missile threats results in higher collision energy for a given Lightcraft mass and speed. That is because the higher entry speed of longer-range missiles contributes more collision velocity (target plus Lightcraft velocity component along the target velocity vector).

This BMD air-to-space mission appears to be more favorable for Lightcraft than air-to-ground/sea or air-to-air missions, which are not considered here because they are beyond the scope of this report. This mission results in higher altitude flight where atmospheric propagation losses of laser beams are lower, and in higher impact velocities for higher Lightcraft impact energy or lower mass. But like air-to-air missions, BMD would require semi-active terminal guidance using uncooled IR detectors and chemical rocket thrusters for end-game maneuvering to ensure hit-to-kill accuracy. It is therefore estimated that the air-to-space Lightcraft dry mass would be about the same as the air-to-air Lightcraft (approximately 2.0 kg). This particular Lightcraft

system, like the air-to-air one, has reduced capability if an enemy can achieve nearly simultaneous arrival times for all of its ballistic missiles. If so, then a Lightcraft BMD system would have to serve as an adjunct to other BMD systems, such as the ground-based PAC-3 Patriot, THAADS, or NMD which are deployed for national or theater ballistic missile defense. However, this system could protect regions against limited ballistic missile attacks at the earliest phase of hostilities before ground-based BMD systems could arrive and be deployed.

Table 4. Influence of Target Velocity and Intercept Angle on Impact Energy and Required Mass [26].

Lightcraft Intercept Velocity	Lighteraft Intereept Aspect	Impact Energy and Weight	Ballistic Missile Threat		
			SRBM R~1000 km V=2 km/s	IRBM R~2500 km V=4 km/s	ICBM R~10,000 km V=6km/s
3 km/s	0° from Head-on Collision	Impact E for 1.0 kg Wt.	25 MJ	49 MJ	81 MJ
		Wt for 10 MJ of E	.40 kg	.20 kg	.12 kg
	30° from Head-on Collision	Impact E for 1.0 kg Wt.	21 MJ	44 MJ	74 MJ
		Wt. For 10 MJ of E	.47 kg	.23 kg	.14 kg
	45° from Head-on Collision	Impact E for 1.0 kg Wt.	17 MJ	37 MJ	66 MJ
		Wt. for 10 MJ of E	.59 kg	.27 kg	.15 kg

Table 5. Influence of Lightcraft and Target Velocity on Impact Energy and Required Mass [26].

Lightcraft Intercept Aspect	Lightcraft Intercept Velocity	Impact Energy and Weight	Ballistic Missile Threat		
			SRBM R~1000 km V=2 km/s	IRBM R~2500 km V=4 km/s	ICBM R~10,000 km V=6km/s
0° from Head-on Collision	2 km/s	Impact E for 1.0 kg Wt.	16 MJ	36 MJ	64 MJ
		Wt for 10 MJ of E	.63 kg	.28 kg	.16 kg
	3 km/s	Impact E for 1.0 kg Wt.	25 MJ	49 MJ	81 MJ
		Wt. For 10 MJ of E	.40 kg	.20 kg	.12 kg
	4 km/s	Impact E for 1.0 kg Wt.	36 MJ	64 MJ	100 MJ
		Wt. for 10 MJ of E	.28 kg	.16 kg	.10kg

RECOMMENDED LIGHTCRAFT MISSIONS FOR BALLISTIC MISSILE DEFENSE

Laser-powered Lightcraft, flown on air-to-space trajectories, show much promise for performing exo-atmospheric BMD missions, especially if the laser can also be used to discriminate warhead-carrying vehicles from decoys and non-threatening debris. Such Lightcraft also appear capable of eliminating enemy satellites in LEO, if the Lightcraft laser can illuminate them. But a significant effort would be required to analyze the engagement scenarios for such a system, and fully investigate the decoy discrimination and satellite tracking capabilities of the Lightcraft's pulsed laser and the hit-to-kill guidance requirements for the Lightcraft itself.

Locating lasers and Lightcraft on existing aircraft, such as the Boeing 747, B-1 Lancer, or C-130, appears to be an attractive alternative to ground/sea-based laser Lightcraft systems. In this case, airborne laser beams at 12 km altitude will not suffer the significant propagation losses that occur when guiding and propelling Lightcraft through the lower atmosphere, and greater Lightcraft flight range should therefore be achievable. (The increase in laser range, due to reduced propagation losses, for high altitude operation will be somewhat diminished because of the smaller allowable apertures on aircraft-mounted laser optics, which are on the order of 1.0 m as compared to apertures on the order of 10.0 m for large ground/sea-based laser installations.) Furthermore, airborne laser Lightcraft systems possess much greater operational flexibility since their carrier aircraft can fly over significant distances to reach desired launch locations, and can be based at almost any major Air Force facility

that has runways of reasonable length. An air-launched Lightcraft launch vehicle mission, involving the transport of lasers and Lightcraft on medium-sized bombers or transport aircraft, is also recommended if additional funding would become available.

FUTURE NANO-/PICO-SATELLITE MISSION CONCEPTS

Coherently cooperating "swarms" are a novel innovation for replacing structures with information by placing many formation-flown small satellites into a loose "swarm" and cause them to cooperate coherently. This is very different from the so-called distributed small satellite LEO constellations currently pursued in which individual small spacecraft perform essentially the same functions as larger satellites but at lower spacecraft mass (or weight) and cost. These smaller spacecraft can be proliferated to provide greater geographical coverage for the same cost. The lower mass also saves launch costs, so the total system costs less for the same function performed with larger spacecraft.

In contrast, the swarms, as described in the following sections, cooperate coherently and form a real distributed system in which the whole is more than the sum of the parts. A generic description would be a constellation of small spacecraft each performing its separate function, but these functions combine to create at a central location a much larger virtual spacecraft, or sensor aperture, that exists solely because of the cooperation of the spacecraft. The following sections provide several examples of the implementation of such systems in which each of a large number of small satellites in a swarm or other constellation will radiate or receive signals and combine them in phase, or coherently, regardless of their actual location in orbit. This creates coherent RF or optical apertures that are essentially unlimited in size.

Each satellite's position is only crudely station kept, and the satellites adjust the time delay or phase delay of the signals they repeat to compensate for their position errors, causing their repeated signals to add coherently at a collection point. This technique can be easily applied to RF transmitters and receivers, and with more demanding accuracy to optical transmitters and receivers. The result in either case is a large "swarm" or loose constellation of satellites that act as one large antenna or optical array, even though they are separate and their positions are neither constant nor lie along a parabola or plane in space. The individual satellites can be as simple as one-element flying chips or as complex as today's self-contained sensing spacecraft of various sizes.

The advantage of coherently cooperating distributed systems is that they can form sparse RF antennas and optical sensors with diameters so large that they would be impossible to implement with filled apertures even if formed with adaptive membranes; and have orders of magnitude smaller mass. The relative locations of individual spacecraft in the swarm can be controlled by MEMS FEEP propulsion, tethers, or by cleverly conceived orbits in which the elements of the array appear to orbit a common center within it, thus eliminating the need to use propulsion at least for first order station keeping.

36

These array functions can be made coherent over very great distances. RF antennas with sizes of hundreds of kilometers and optical telescopes of hundreds of meters diameter can be formed. These systems can enable new capabilities not possible with single spacecraft either acting alone, as a proliferated but non-coherent constellation, or as relays for each other. Formed of nanosats and picosats, such swarms will contain so many spacecraft that the economics of true mass production will come into play in space for the first time, greatly reducing the cost of producing the system. In addition, these systems feature the advantages of truly distributed satellite systems, including fault tolerance, robustness, survivability, reconfigurability by software, and the ability to be incrementally emplaced and upgraded as budgets are available.

These swarms can be implemented in a cost effective manner using laser propulsion for both launch and orbital insertion. However, the system designs described in the following sections are flexible enough to allow for the use of alternative conventional launch vehicle technologies. The technologies to produce these swarms and their constituent nanosats or picosats probably can be demonstrated by 2015 and deployed in space by 2020.

The following concepts were provided via the voluminous research notes, lectures, and briefings provided courtesy of I. Bekey.

ROTATING PICOSAT SWARM ARRAY RADIO FREQUENCY COLLECTOR

An unconventional, large sparse antenna array RF collector spacecraft with a small surface footprint even when deployed in geosynchronous Earth orbit (GEO) separates different sources in proximity and also detects weak signals. Its implementation would result in a highly desirable, long dwell RF emitter detection capability.

At the heart of this system is a large antenna that is formed by a swarm of tiny elements that make up the lens of a space-fed array with no structure. The antenna is a sparse, self-cohering array formed from a large number of picosats rotating (in relative coordinates) in a plane around a central orbital point in GEO. The picosats are self-contained repeater spacecraft. Each one receives the ground signal, delays it, and retransmits the signal so that it arrives at the feeds at the same time as a direct ray through the center of the array. The time delay of each picosat is self computed based on its location in the swarm, as measured by a local differential global positioning system (DGPS)-like navigation signal, to compensate for its deviation from its assigned ideal location. Each picosat digitizes, delays, frequency shifts, and retransmits its received signals independently, causing an in-phase composite signal from the ground to be received at the feeds.

The relative positions of these picosat elements change slowly, and only small and infrequent propulsive maneuvers are needed for constellation maintenance. A tether along the local vertical at the central point holds the receivers and DGPS-like reference at the focus against a counterweight. A pseudorandom distribution of the picosats suppresses the antenna grating lobes, and intensive computation greatly reduces much of the remaining sidelobes, creates multiple beams, and steers the ensemble of the individual beams anywhere on Earth. The antenna system will function with far fewer elements as a more sparse array, though with limited sensitivity. This system can be

37

incrementally emplaced, upgraded, and even funded with capability growing as budget is available, as opposed to the usual all-or-nothing functioning of today's spacecraft.

The antenna size is 20 km × 40 km and contains 150,000 picosats, each of which weighs 23 grams. The feed array is held in position by a 50 km long, lightweight tether against a counterweight. There is no truss or other structure. Each picosat is gravity-gradient stable, has a dipole array facing Earth, and a broader beam antenna array facing the receivers.

The effective collecting aperture of the array is equal to that of an equivalent 80 m diameter filled aperture antenna. The coverage spot diameter can be varied by choosing the diameter of the array that is active, with spot sizes on Earth as small as 30 m at 10 GHz, 300 m at 1 GHz, or 3 km at 100 MHz. It can receive sub-watt signals from individual cell phones. The entire constellation weighs 3,500 kg, but that could be reduced in the future to 35 kg if Buckytubes are used to construct the system.

HIGH RESOLUTION SURFACE SAMPLING RADIOMETRY

Highly sensitive radiometry at low microwave frequencies with a small ground foot-print would result in high resolution microwave radiometry sampling maps of soil moisture and other surface characteristics, as well as passively detected larger targets. The constellation/array implementation follows that of the preceding concept (Future Nano-/Pico-Satellite Mission Concepts section), except that it is designed to map the surface radiation rather than detect discrete emitters. The antenna size is 8 km × 12 km and contains 12,000 picosats, each of which weighs 23 grams. The feed array is held in position by a 40 km long, lightweight tether against a counterweight. The constellation scans its coverage spot electronically in a 1,200 km zig-zag swath from its 4,000 km orbit by modulating the time or frequency shift of the ensemble of picosats. These picosats are similar to those in the Rotating Picosat Swarm Array Radio Frequency Collector section.

The effective collecting aperture of the array is the sum of those of the picosats, and in this example, equal to that of an equivalent 11 m diameter antenna. However, the coverage spot diameter is set by the total aperture diameter of 8 km × 12 km, and thus is 100 m at 1 GHz. Five constellation/arrays would result in a 5 hour global revisit with zig-zag coverage of the scanned swaths. The entire constellation weighs 3,000 kg, but that could be reduced in the future to 30 kg if Buckytubes are used to construct the system.

HIGH RESOLUTION SURFACE MAPPING RADIOMETRY

Highly sensitive radiometry at low microwave frequencies with a very small foot-print on the ground would result in high resolution microwave radiometry maps of soil moisture and other surface characteristics and passively detected larger targets, with 100% of Earth's surface mapped with a 5 hour revisit time. The principle of operation is the same as that of the previous concept (High Resolution Surface Sampling Radiometry section), except that a multiple element detector array is used in a

38

pushbroom scanning mode for complete Earth coverage rather than only sampling coverage.

The constellation/array implementation is similar to that of the preceding concept (High Resolution Surface Sampling Radiometry section), except that tethers hold a receiving array that must be 2 km long to obtain the 1,200 km instantaneous swath width with a resolution of 100 m. It consists of a 2 km long focal surface with 12,000 printed dipoles, shaped into a focal surface by gravity gradient forces balanced against magnetic forces from a superconducting conductor around its periphery, acting on a piezoelectric, electron beam-shaped, adaptive membrane substrate. The large antenna is formed by a swarm of tiny elements making up the lens of a space-fed array.

The antenna is a 4 km × 6 km diameter, sparse, self-cohering array formed from 12,000 picosats weighing 23 grams each, rotating in relative coordinates in a plane around a central orbit point. The picosats are similar to those of the preceding concept (High Resolution Surface Sampling Radiometry section). Their locations are initially selected to lie in a plane, and their spacings are pseudorandom to minimize the sidelobe levels, with each picosat designed to loosely stationkeep inside a box 10 m on a side. The relative positions of these picosat elements changes slowly, and only small and infrequent stationkeeping propulsive maneuvers are needed for constellation maintenance.

The effective collecting aperture of the array is the sum of those of the picosats, and in this concept, equal to that of an equivalent 6 m diameter antenna at 2 GHz. However, the coverage spot diameter is set by the total aperture diameter of 4 km × 6 km, and thus is 100 m at 2 GHz from a 4,000 km orbit. Five constellation/arrays would produce 100% global coverage with 5 hour revisit for time critical measurements. The entire constellation weighs 3,000 kg, but that could be reduced in the future to 30 kg if Buckytubes are used to construct the system.

ROTATING NANOSAT SWARM DISTRIBUTED RADAR

An extremely powerful space-based radar, this concept would allow detection of most air, land, sea, and space targets, as well as many "low observable" targets anywhere, with one or a few constellations in GEO. A large, sparse array antenna using a swarm of nanosats creates a space-based radar system. The constellation/array implementation is similar to that of the preceding rotating swarm concepts, except that it generates and radiates extremely large peak and average powers, and given the generally high angles of viewing can detect and track many air, space, and surface targets from GEO.

The constellation is composed of 10,000 nanosats that are self-contained repeater spacecraft weighing about 1 kg each. Each nanosat receives the ground signal, digitizes, delays, and retransmits it, causing it to arrive at the feeds at the same time as a direct ray through the center of the array. The time delay of each nanosat is self computed based on its location in the swarm, as measured by a local DGPS-like navigation signal, to compensate for its deviation from its assigned ideal location. Commands for beam sweep delays are superimposed on the time delays of each nanosat. Each nanosat generates 10 W of average power and 10 kW peak power at

0.001 duty cycle, has a helical film antenna that increases its gain and doubles as a solar sail for infrequent stationkeeping maneuvers, and has a tether for coarse gravity gradient stabilization. A 50 km tether supports the feed, transmitter, and DGPS reference assembly against a counterweight. The antenna lens is 2 km × 4 km.

The effective area of the array is the same as that of a 50 m diameter filled aperture. The total effective RF radiated power of the system is 3 GW peak and 3 MW average. Although specific performance calculations have not been done for this concept, these powers are so large that the radar should have the sensitivity from its location in GEO for detecting and tracking many targets simultaneously and most "low observable" targets as well because they are all designed and oriented so as to have their low observables in near-horizontal directions. Three constellations would provide essentially complete global coverage. The entire constellation weighs about 11,000 kg in GEO (this could be reduced in the future to 110 kg if Buckytubes are used to construct the system) and can be emplaced and replaced incrementally using laser-powered Lightcraft launch vehicles or even small conventional launch vehicles. It could even be funded incrementally.

Simple, Distributed, Hyperspectral Sensor

This concept presents an unconventional method of implementing a hyperspectral sensor of great spectral and spatial resolution. Its implementation would allow the detection of very many spectral intervals simultaneously, and it has a small field of view from GEO so that the instrument can dwell on and resolve particular targets of interest. It also has a large field of regard so that one spacecraft covers a significant fraction of a hemisphere.

The concept uses a Fresnel zone plate, which is oriented roughly parallel to the local horizontal just below GEO. It is supported by a tether that extends well above the GEO altitude, and may or may not have a counterweight at the top end. The gravity gradient causes the ensemble to remain Earth pointing along the local vertical, with its center of mass in GEO.

The Fresnel zone plate has a long focal length, and thus the surface and ring locations can be imprecise compared with conventional optics. In addition, the lens is a thin film membrane and will be light and inexpensive. It is highly frequency dispersive, and thus its focal length is a sensitive function of wavelength. Small, self-contained optical sensor nanosats are placed on the tether at many locations with each nanosat's optics filtered for response at only that narrow spectral region focused at its distance from the lens. The nanosats can transmit directly to the ground or their signals can be combined in one transceiver, also on the tether.

This system has a 100 km long tether, which weighs only a few kilograms in GEO. The Fresnel zone plate is 100 m in diameter, has a collecting aperture equivalent to a 30 m filled aperture, and requires only a surface accuracy of centimeters in the visible light region. It is constructed of thin film with deposited aluminum rings and is an adaptive piezoelectric membrane kept flat by an electron beam in response to an optical figure sensor. MEMS FEEP thrusters are at the sensor's periphery for attitude control, with

1,000 nanosats attached to the tether. Each nanosat is a self-contained optical sensor spacecraft, integrated into a 0.1 kg package. The sensor thus detects 1,000 wavelengths simultaneously. The sensor has a resolution as small as 40 cm on the ground from GEO. Its field of view can be scanned over an area by tilting the ensemble using MEMS FEEP thrusters on the nanosats, or libration modes can be excited in the tether so that the field of view scans across a 2,000 km coverage area in a quasi-random mode, eventually covering the entire area. These thrusters also serve for stationkeeping. Its total weight is less than 900 kg in orbit, which can be reduced in the future to 9 kg if Buckytubes are used to construct the system.

Chapter 4: Summary of Multi-Megawatt Laser Study for Lightcraft Propulsion Applications

SUMMARY OF LASER STUDY PERFORMED BY TEXTRON SYSTEMS

In 2002, V. Hasson (TEXTRON Systems Corporation) conducted a study of candidate multi-megawatt laser systems for laser Lightcraft propulsion [29].

Candidate high-power/high-energy lasers identified in the study:

- Carbon Dioxide (CO_2) Laser: technical issues include large wavelength and atmospheric absorption of the laser beam.
- Carbon Monoxide (CO) Laser: technical issues include large wavelength, atmospheric absorption of the laser beam, and toxicity of the lasing fuel (CO gas).
- Hydrogen Fluoride (HF) or Deuterium Fluoride (DF) Laser: technical issues include atmospheric absorption of the laser beam, corrosive lasing fuel chemicals, pulse energy, running cost, and beam quality.
- Chemical Oxygen-Iodine Laser (COIL): technical issues include fuel chemicals, pulse energy, and running costs.
- Bulk Slab Solid-State Laser (BSSSL): technical issues include cost, average power, and run duration.

The first four gas dynamic and chemical laser candidates have already demonstrated megawatt-class average beam output power. The study then reviewed the development, testing and operational legacy of the first candidate laser technology, which included a review of the various system architectures that use other gas mixtures combined with CO_2. The study recommended a new design for a 10 MW (beam output power) electron gun-driven CO_2/gas mixture laser because this technology does not require additional R&D and can be implemented now. The other gases selected for the lasing fuel are N_2 and H_2, which, in combination with CO_2, offer superior performance over systems using helium.

However, very recent technologically disruptive innovations led to the 10-fold increase in the beam output power of bulk slab SSLs and their newly emergent solid-state cousin, called high-power fiber lasers, which has made these devices more competitive with high-power chemical and gas dynamic lasers on the basis of average beam power, peak beam power, electrical wall plug and optical efficiencies, cost, complexity, mass, and size. Free-electron lasers are another class of laser technology that was not reviewed by Hasson, but recent technological innovations are accelerating their development to the point where their present average beam output power of 20 kW will be increased to 100 kW or higher within the next 12 to 24 months following the publication of this report. The output beams of several of these laser devices can be optically combined to produce a single beam with megawatt-class average output power. It is for this reason that we will summarize their technology in Summary of Emergent High-Power Solid-State and Free-Electron Laser Technologies section.

An outline of the conceptual design features of the proposed 10 MW electron gun-driven CO_2/gas mixture laser is [29]:

- Scalability of total beam output power, beam combining concept.
- Power oscillator or master oscillator-power amplifier (MOPA) design.
- Unstable optical resonator cavity with grating and rotating mirrors beam-combine techniques.
- Flow and gas handling system with blow down and exhaust to the atmosphere.
- Acoustics suppression with expansion horn downstream and anode muffler.

In this concept there are four separate laser transmitters each generating 2.5 MW output beams that are combined into a single 10 MW output beam. The oscillator parameters for each beam transmitter are [29]:

- Energy loading, E_p: E_p = 300 J (higher loadings at reduced gas temperature); gain volume = 0.27 m^3 ($\times$ 4 lasers); A to K = 0.3 m; gain length = 3 m.
- Specific laser output = 65 J/I.
- Estimated extraction efficiency = 20%.
- Pulse repetition rate: 125 Hz @ 20μs.
- Laser power, P = 2.5 MW/beam $\times$ 4 beams = 10 MW.
- Laser energy per pulse = 18 kJ/beam x 4 beams = 72 kJ.
- Output wavelengths: 10.6 μm, 10.2 μm, 9.6 μm, and 9.3 μm (mixed).
- Gas mixture ratio (for N_2:CO_2:H_2): 3:1:0.08.
- Gas pressure = 1.013 $\times$ 10^5 Pa (or 1 atmosphere).
- Flash factor = 1.3.

The optical resonator cavity and optical components specifications are [29]:

- Resonator type: confocal unstable with rotating mirrors beam combining.
- Magnification, M = 4.
- Cavity length, L = 36.5 m.
- Equivalent Fresnel number = 3.4.
- Cavity end mirrors radius of curvature: $R_{Mirror1}$ = 97.3 m (concave), $R_{Mirror2}$ = 24.3 m (convex).
- Gain cell: volume = 0.3 $\times$ 0.3 $\times$ 3.0 m^3, length = 3 m.
- Beam combine mirrors: 75 $\times$ 75 cm^2 flat (30 x 30 cm^2 apertures) @ λ = 10.59 μm.
- Low pressure hot cell: 0.3 to 0.5 GHz suppression near line center.
- Output scraper mirror: D = 0.075 m (taped).

See Figure 16 and Figure 17 for schematics of the power oscillator optics and the MOPA. The laser operation requirements for the gas flow system are (see Figure 18) [29]:

- Flow System: blow down.
- Gain Section
  - Cross-section, A = 0.3 m $\times$ 3.0 m = 0.9 m^2.
  - Volume, V = 0.3 m $\times$ 0.3 m $\times$ 3.0 m = 0.27 m^3.
  - Flow speed, u = 50 m/sec (@ 125 Hz & flash factor = 1.3).
  - Dynamic pressure, ΔP = 2000 Pa (or 0.02 atmospheres).
  - Mass flow rate, Q = 60 kg/sec per module (45 m^3/sec std).
  - Run time, t = 300 seconds

43

- Total mass flow rate, Q_{total} = 240 kg/sec [for a total (run time) mass of 72 metric tons].
- Plenum Chamber
  - Volume, V = 0.5 m × 3.0 m × 1.5 m = 2.25 m³.
  - Static pressure, P = 2.02 × 10⁵ Pa (or 2 atmospheres).
  - Sonic orifice plate perforation = 17.5%.
  - Flow screen loss > 0.2 to 0.3.
  - Skin friction loss ~ 0.08.
- Gas Storage Tank
  - Run time = 300 seconds & 4 to 5 runs.
  - Pressure, P = 2.066 × 10⁷ Pa (or 200 atmospheres).
  - Volume, V = 68 m³ × 4.
- Acoustics Suppression
  - Pumping induced medium homogeneity, $\Delta P/P$ = 0.94 @ E_p = 300 J/l.
  - Acoustic suppression
    - Flow direction: expansion horn provides impedance match eliminating reflection of pressure waves.
    - Normal to flow direction: using acoustics muffler to dump out transverse pressure waves.
    - Muffler requirements: attenuation factor < 0.55; number of bounces between pulses n = 8.
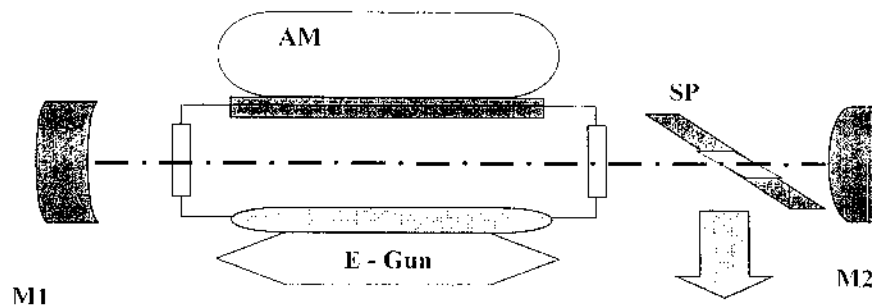
End Mirrors : M1 Concave (R1 =97m)
            M2 Convex (R2=24m)
Magnification : M=4
Output Scraper: SP 36x36 cm (outer)
                7.5x7.5 cm (inner)
Acoustic Muffler : AM
Electrodes : E

Cavity Length : 36.5m
Gain Length : 3m
Aperture : 0.3x0.3 m

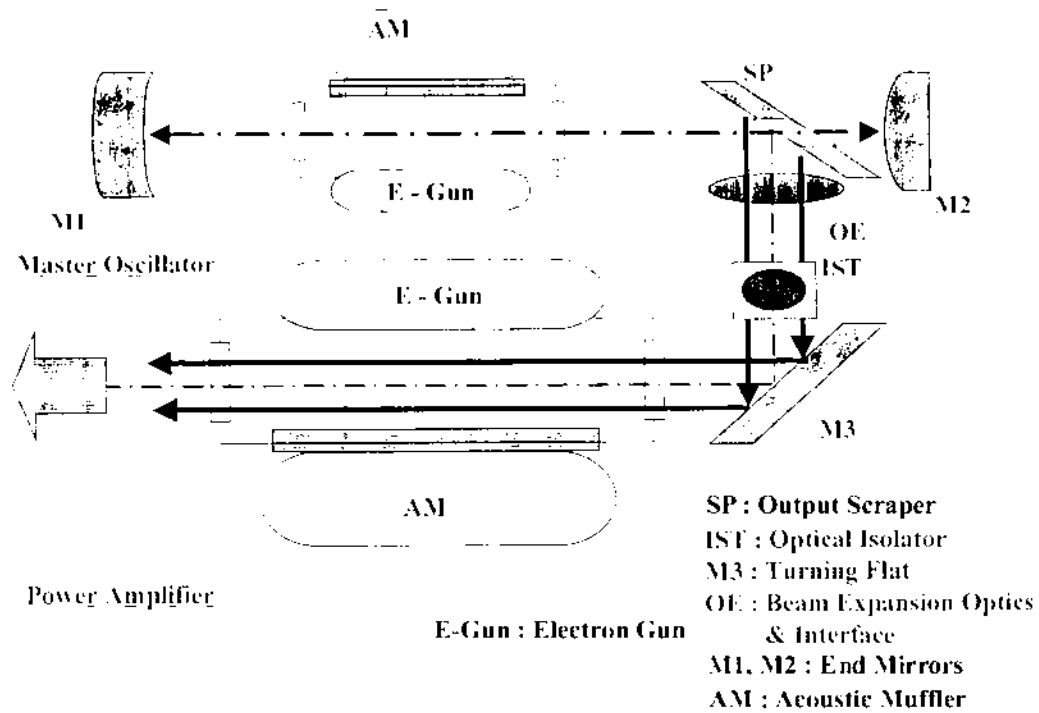**Figure 16. Schematic of Power Oscillator Optics** [29].
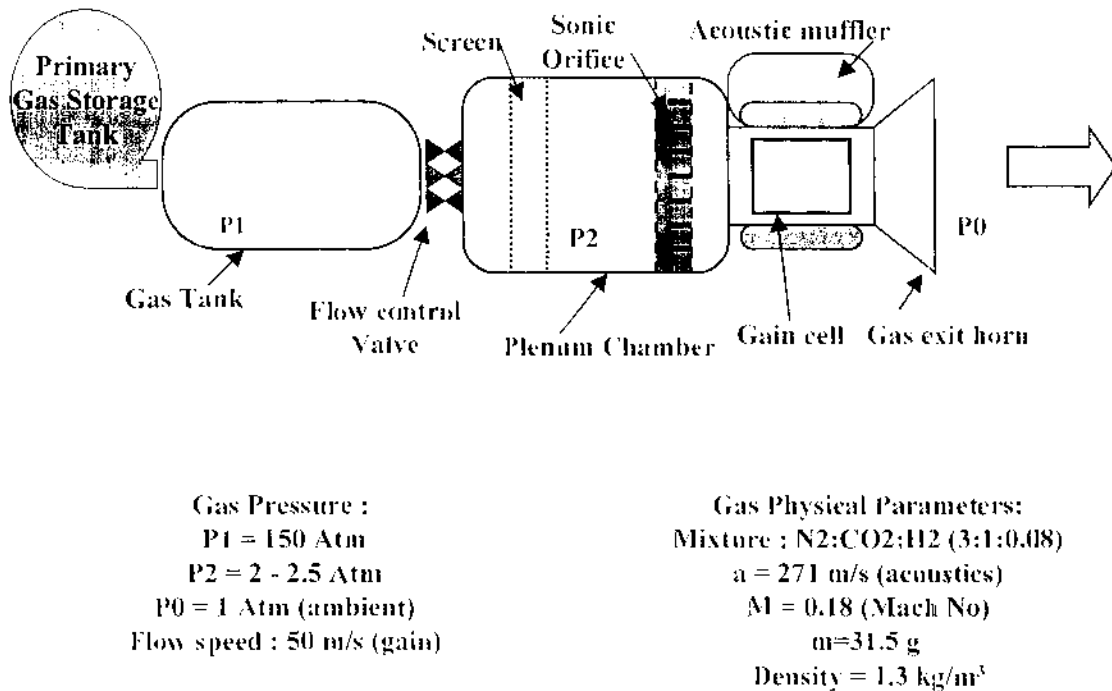
Figure 17. Schematic of MOPA [29].

Gas Pressure :
P1 = 150 Atm
P2 = 2 - 2.5 Atm
P0 = 1 Atm (ambient)
Flow speed : 50 m/s (gain)

Gas Physical Parameters:
Mixture : $N_2:CO_2:H_2$ (3:1:0.08)
a = 271 m/s (acoustics)
M = 0.18 (Mach No)
m=31.5 g
Density = 1.3 kg/m^3

Figure 18. Schematic of the Laser $N_2/CO_2/H_2$ Gas Flow System [29].

45

The total cost for an installed 10 MW power oscillator-based laser transmitter is estimated as follows [29]:

- 2.5 MW Prototype = $80.0 Million.
- 3 × 2.5 MW Additional Modules + 4 Module Integration = $133.0 Million.
- Buildings/Installations ~ $17.0 Million.
- Total Installed & Integrated Transmitter Cost ~ $230 Million.

And the additional costs for the MOPA-based transmitters and cold-flow assessment are [29]:

- 4 Master Oscillators ~ $20.0 Million.
- Cold-Flow Subscale Upgrades & Evaluations ~ $5.0 Million.
- Total Additional Cost ~ $25.0 Million.

The TEXTRON Systems study concluded that [29]:

- A pulsed CO_2 repetitively pulsed transmitter, which uses a 300 second blow down and beam combining, can provide the power levels and energies needed for Lightcraft propulsion applications.
- Spectral tailoring of the beam and mountain-top operation should provide reasonable atmospheric transmission of the high pulsed-power laser beam.
- Low cost operation is achievable with helium-free gas mixtures, which use N_2, CO_2, and small quantities of H_2.
- Subscale testing will be used to anchor the design and thus reduce risk.
- Legacy programs support many aspects of this approach.
- Growth potential with cold-flow and aero windows should double the beam power output.
- Current pulsed CO_2 laser technology blow down configuration is postured to provide power levels for propulsion of kilogram-sized spacecraft into orbit.

Payload Cost Estimate for Lightcraft Launch Using a 10 MW CO_2/Gas Mixture Laser

Froning and Davis [26] used a proposed 10 MW electron gun-driven N_2/CO_2/H_2 laser design to estimate the Lightcraft payload launch cost per kilogram, which is described in what follows. Each power oscillator optics module transmitting a 2.5 MW beam of 10.6 μm wavelength photons generates 1.334×10^{26} photons/sec, and 15 kg/sec of CD_2 mass flow represents 2.053×10^{26} molecules/sec of gas flow. These figures taken together mean that 1.54 CO_2 molecules are required to lase one photon. A 2.5 MW laser operating for 300 seconds of thrusting will allow us to send 5.25 kg of payload into LEO, and the total laser energy (E_{laser}) output is 750 MJ. If the laser efficiency is 0.20, then we will need to use 12.5 MW of electrical power for 300 seconds (or 3,750 MJ of total energy), which, at a cost of $0.10 per kWh (or $0.0278 per MJ), gives a total cost of $104 for the required electrical energy to launch the payload.

The kinetic energy (K_E) of a Lightcraft in LEO is given by $K_E = \eta\alpha\beta\gamma E_{laser}$, where [26]:

- $\eta = 1$: this is the conversion efficiency of laser rocket propellant-thrust-jet K_E into vehicle K_E, in which the propellant/laser is designed so that the rocket thrust-jet velocity is equal to the vehicle velocity throughout the mission, i.e., the laser rocket has variable $I_{sp} \approx 100$ seconds at beginning of mission to 1000 seconds at end of mission;
- $\alpha\beta = 0.5$: α is efficiency of laser energy absorption and β is efficiency of conversion of propellant internal energy into thrust-jet K_E;
- $\gamma = 0.7$: this is the atmospheric transmission efficiency;
- $E_{laser} = 750$ MJ.

These numbers multiplied together give a vehicle $K_E = 262.5$ MJ in LEO. If the effective change in velocity (Δv) required to get to LEO is 10 km/sec (8 km/sec orbital velocity + 1 km/sec for gravity + 1 km/sec for drag loss), then 1 kg in LEO has 50 MJ of energy investment and a 5.25 kg payload in LEO has 262.5 MJ of energy investment.

The 60 kg/sec mass flow requirement of the 3:1 N_2/CO_2 lasing gases means that a mass flow of 15 kg/sec of CO_2 and 45 kg/sec of N_2 is required. For the 300 seconds of thrust we will therefore need 4.5 tons of CO_2 and 13.5 tons of N_2 gases (we are neglecting the tiny amount of H_2) to launch a payload to LEO. Liquid CO_2 costs $100 per ton and liquid N_2 costs $154 per ton. The total lasing gas cost is therefore $450 for the liquid CO_2 and $2,079 for the liquid N_2. Adding these two gas fuel costs to the $104 cost of the required electrical energy gives a total of $2,633 to launch a 5.25 kg payload to LEO. This result represents a cost of $501 per kg of payload (or $228 per pound) launched to LEO, which is 44 times lower than the oft-quoted standard space launch industry cost of $10,000 per pound for conventional chemical propulsion rockets systems.

However, this cost figure needs to be slightly adjusted to account for other factors. If we use the N_2/CO_2 gases at a temperature of 217 K in the laser, then we will have to boil the liquid CO_2 and the liquid N_2 with additional heating of the gaseous N_2. Boiling 4.5 tons of liquid CO_2 at 217 K requires 1,175 MJ of energy, boiling 13.5 tons of liquid N_2 at 77 K requires 2,683 MJ of energy, and heating the 13.5 tons of gaseous N_2 from 77 K to 217 K requires 1,890 MJ of energy. Therefore, the additional energy required to prepare the laser gases is 5,748 MJ (= 1,175 MJ + 2,683 MJ + 1,890 MJ), which represents an additional electricity cost of $160. Adding this additional energy cost to the previous total of $2,633 gives a *final total cost* of $2,793 to launch a 5.25 kg payload to LEO. This new final result represents a cost of $532 per kg of payload (or $241 per pound) launched to LEO, which is 41 times lower than the space launch industry cost of $10,000 per pound for conventional chemical propulsion rockets. Note that this final cost estimate *excludes* the operations, life-cycle, and maintenance costs that are listed in Table 1, which were based on the use of a bulk solid-state laser.

SUMMARY OF EMERGENT HIGH-POWER SOLID-STATE AND FREE-ELECTRON LASER TECHNOLOGIES

Bulk Slab Solid-State Laser

Under the auspices of the Joint High Power Solid-State Laser (JHPSSL) program, Northrop Grumman broke the all-important 100 kW beam power threshold in early 2009 by firing a 7-amplifier chain bulk slab solid-state laser (BSSSL) that produced a beam output power of almost 106 kW (see Figure 19). Each amplifier chain is assembled with several high-gain power modules. The laser operated for more than five minutes, achieved electro-optical efficiency of 19.3%, and reached full power in less than 0.6 seconds with a beam quality of better than 3.0, Whereas the test demonstration saw five minutes of continuous operation for the laser, altogether the system has been operated at above 100 kW beam power for a total duration of more than 85 minutes. Adding an eight amplifier chain that the system was designed for will increase the beam power to 120 kW.
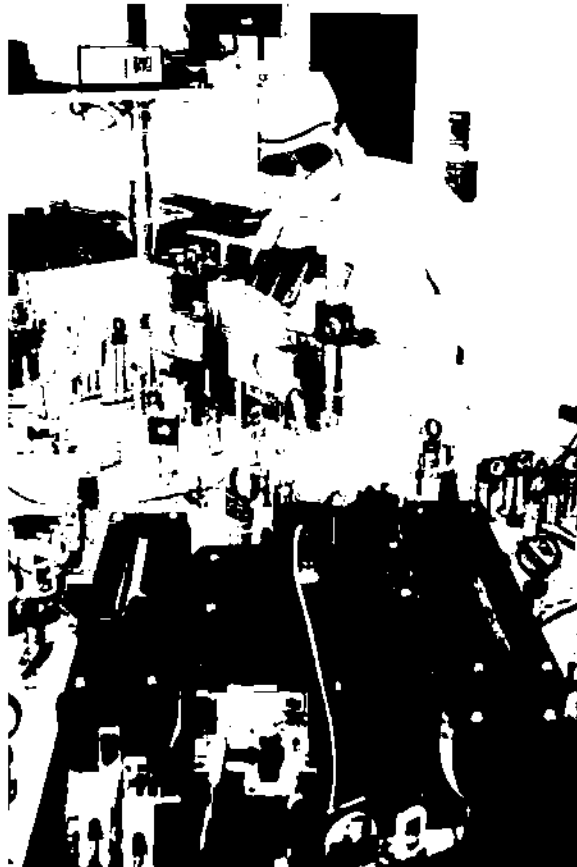

Figure 19. Northrop Grumman's Joint High Power Bulk Slab Solid-State Laser (courtesy of the Directed Energy Professional Society).

Even though 100 kW beam power has long been the proof-of-principle sought for weapons-class lasers, it should be noted that many militarily useful effects can be

achieved by laser weapons with 25 kW or 50 kW beam power, provided the energy is transmitted with good beam quality. Laser propulsion requires megawatt-class lasers which are only developed in directed energy weapons (DEW) programs. However, BSSSL beam power can be scaled up further by improving presently known gain media and doping combinations, inventing new gain media and doping combinations, by combining the beams of several lower-power devices, or a combination of all these until the ultimate optical/thermal/mechanical limit of slab gain materials is reached. BSSSL beam output power is projected to reach the multi-megawatt level within three to five years from the time of this writing (P. Zarubin, J. Albertine, and V. Hasson, private communications, 2010).

Figure 20 shows DARPA's High Energy Liquid Laser Area Defense System (HELLADS) as an example of a liquid-cooled bulk slab solid-state (ceramic) laser. HELLADS is designed to be light and compact enough to fit on a jet fighter or drone aircraft, and yet powerful enough to fire a 150 kW beam of energy. HELLADS makes use of a unique cooling technique to save weight and size. The high-power laser uses a liquid that has the same index of refraction as the mirrors inside the laser. That way, the laser can fire away, even while it's being cooled. The HELLADS program will deliver a 150 kW laser weapon at 2 m^3 of system volume and 600 kg of system mass (not including the prime power and cooling systems) to achieve the low specific mass (5 kg/kW) and compact size need to be mounted on small tactical airborne platforms like the C-130 transport, jet fighters, or Predator-class UAVs. The device will be built by General Atomics and the tracking system will be built by Lockheed-Martin.

A bulk solid-state laser is based on a bulk piece of doped crystal, disordered or amorphous material (such as glass), glass ceramic (which is a combination of crystalline-ordered structure and glassy phases disordered structure), or mixed crystals as the laser gain medium. In most cases, the gain medium is doped either with rare-earth ions or transition metal ions. Typically, these ions replace a small percentage of other ions of similar size in the host medium. The laser-active ions have suitable optical transitions for pumping and laser emission at wavelengths where the host medium is transparent. A bulk laser resonator is often formed with laser mirrors placed around the gain medium. However, there are also laser gain media with a highly reflective dielectric mirror coating on one side, which serves as a resonator end mirror. Also, there are monolithic solid-state lasers where the beam path is entirely inside the gain medium. See Reference 30 for additional technical details.
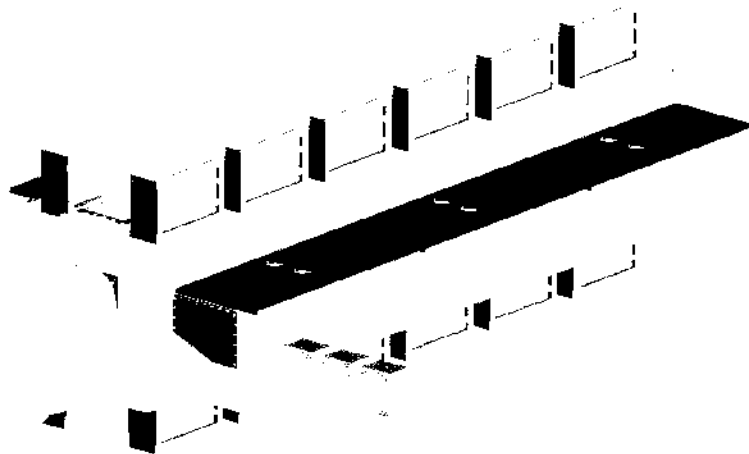
Figure 20. DARPA's High Energy Liquid Laser Area Defense System (courtesy of P. Saunders, AFRL/RDS, Kirtland AFB, NM).

Unlike chemical and gas dynamic laser devices, bulk solid-state lasers possess the following unique characteristics, which make them highly competitive with any chemical or gas dynamic laser systems [30]:

- Reliability.
- High level of safety.
- User-friendly.
- Maintenance-free.
- Low-cost performance, high-volume production.
- Compact size.
- Wide range of wavelength selection and wavelength tunability.
- Variety of power oscillator or master oscillator-power amplifier (MOPA) designs.
- Scalability of beam output power, variety of beam combining techniques: scalable to 1 MW beam power within 2 years.

Typical solid-state lasers have the following technical features [30]:

- Gain medium:
  - Host crystal [e.g., Yttrium Aluminum Garnet (YAG)], glass or ceramic (amorphous materials).
  - Impurity lasing ions deposited (or doped) in host [e.g., Neodymium (Nd^{3+}) or Ytterbium (Yb^{3+})].
  - Range of beam wavelengths (λ) produced: 0.7 μm to > 2 μm.
- Optically pumped with flash lamps or diode lasers.
- Capable of high peak power pulses.

- Average power limited by low thermal conductivity of host material.
- Wavelengths propagate extremely well in clear weather:
  - Very low absorption.
  - Higher scattering.

The requirements for high average power bulk solid-state lasers are [30]:

- Efficient optical pumping of gain medium:
  - Flash lamp or laser diode well matched to absorption band.
  - Small wavelength difference between pump and lasing → low quantum defect.
- Efficient heat removal from gain medium:
  - Improved heat removal techniques from host.
  - Large surface area per unit volume.
  - Or, large volume to store heat with low duty cycle operation.
- Gain medium must retain good (correctable) optical quality.

The typical properties of widely used Nd:YAG lasers are [30]:

- 4 nm absorption line width.
- 24% heating from quantum loss.
- Saturation intensity $\approx$ 3 kW/cm^2 (at $\approx$ 2% dopant).
- Multi-kilowatt average power demonstrated.
- Maximum average power potential $\sim$ several hundred kilowatts:
  - Heat removal makes continuous running a challenge at this power.
  - Current high-energy SSLs produce great amounts of heat (e.g., 600 kW of electrical power in and 100 kW of beam power out equals 500 kW of waste heat).
  - Must store the waste heat and reject it from the system at a lower rate, thus requiring storage and limited duty cycle.
- Quantum defect = pump light photon energy minus laser light photon energy.

The typical properties of widely used Yb:YAG lasers are [30]:

- 18 nm absorption line width.
- Indium gallium arsenide (InGaAs) pump laser diodes at 0.941 μm wavelength:
  - 8.6% heating from quantum loss.
- Saturation intensity $\approx$ 9.7 kW/cm^2 (at $\approx$ 25% dopant).
- Multi-kilowatt average power demonstrated.
- Maximum average power potential is perhaps 5 x Nd:YAG laser.

A new technology that enables the scaling-up of BSSSL beam power is a recently developed thermal management system that is used to remove and store the waste heat produced by BSSSL devices. General Atomics' Advanced Power Systems Division recently announced[*] that it has completed testing of an advanced thermal energy

---

[*]Reported in *Space War Newsletter*, June 7, 2010.

storage device capable of cooling DEW systems. Their 3 MJ device is the first large-scale module capable of storing heat at a high rate as required for DEW systems, and it stores heat at an average rate of 230 kW. Heat is stored in a 35 kg module by melting a wax-type phase change material (see Figure 21). These materials, by themselves, cannot support the high heat transfer rate and must be combined with other materials to enhance their thermal properties in order to make them work. Thermal management is one of the many challenges of the high-power BSSSL devices used in DEW systems, which produce tremendous amounts of waste heat. Rejecting heat from these systems in real time is not practical, making thermal energy storage a necessity.

The cost of BSSSL systems and related infrastructure are becoming competitive with that of the proposed 10 MW electron gun-driven CO_2/gas mixture lasers. BSSSL costs are continuously decreasing as their technology matures and as more systems become widely available for testing and operational deployment. The HELLADS matched-index-of-refraction liquid cooling technique and General Atomics' advanced thermal energy storage device will also dramatically improve the cost competitiveness of BSSSL systems compared to all chemical and gas dynamic laser systems by producing greater efficiencies in solid-state lasing operation while at the same time increasing the average beam power.

Figure 21. Phase Change Materials Allow Storage of Large Intermittent Heat Loads While Slow Regeneration Removes Heat from Aircraft (courtesy of P. Saunders, AFRL/RDS, Kirtland AFB, NM).

High Power Fiber Laser

From 2006 to 2009, a newly emergent class of solid-state lasers, called high-power fiber lasers (HPFLs), has undergone transformational innovations resulting in a 10-fold increase in near diffraction-limited beam output power of a single-fiber laser operating with broadband output in the 1 µm wavelength region with 90% optical efficiency, >

30% wall plug efficiency, and pulse repetition rates ranging from a few kHz to 1000 kHz. This exponential growth in beam output power is the result of many factors, including the parallel development of efficient, narrow-band pump diode lasers; and the development of novel fiber geometries such as double-clad fibers and photonic crystal fiber cores (a.k.a. photonic crystal fibers). At present, HPFLs for industrial use routinely achieve 50 kW to 70 kW of beam power, and such systems have already been modified for weapons applications with a goal toward achieving > 100 kW of beam output power within 18 to 24 months after the publication of this report.

As fiber beam output power continues to increase exponentially, individual fibers can be combined coherently for increasing the total beam output power well beyond what has already been achieved by BSSSLs while providing several advantages. HPFLs have several advantages over BSSSLs. They are more efficient, easier to cool due to the large surface area-to-volume ratio, more durable, smaller and lighter, more easily allow the beam to be directed to the target, and have excellent beam quality. Fiber lasers also benefit from economies of scale and are relatively inexpensive devices.

HPFLs possess the following unique characteristics, which make them very highly competitive with any chemical, gas dynamic, or bulk solid-state laser systems [31]:

- Reliability.
- High level of safety.
- User-friendly.
- Maintenance-free.
- Low-cost performance, high-volume production.
- Compact size and low weight.
- Wide range of wavelength selection and wavelength tunability.
- Excellent beam quality and stability.
- Very high wall plug and optical efficiencies.
- Variety of power oscillator or master oscillator-power amplifier designs (see Figure 22).
- Scalability of beam output power, variety of fiber beam combining techniques: scalable to 1 to 2 MW beam power within 1 to 2 years (see Figure 23).

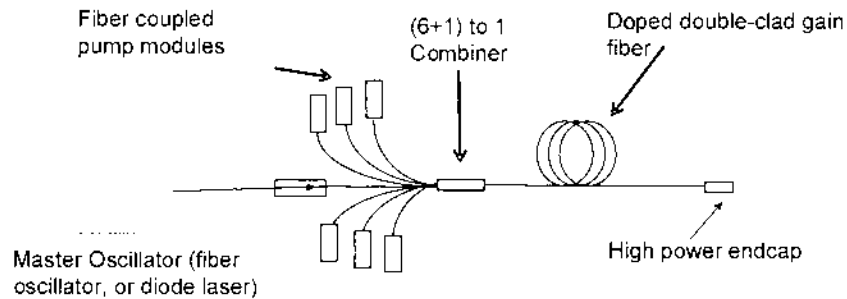# Master Oscillator, Power Amplifier (MOPA)

Figure 22. Typical HPFL MOPA Design (courtesy of the Directed Energy Professional Society).
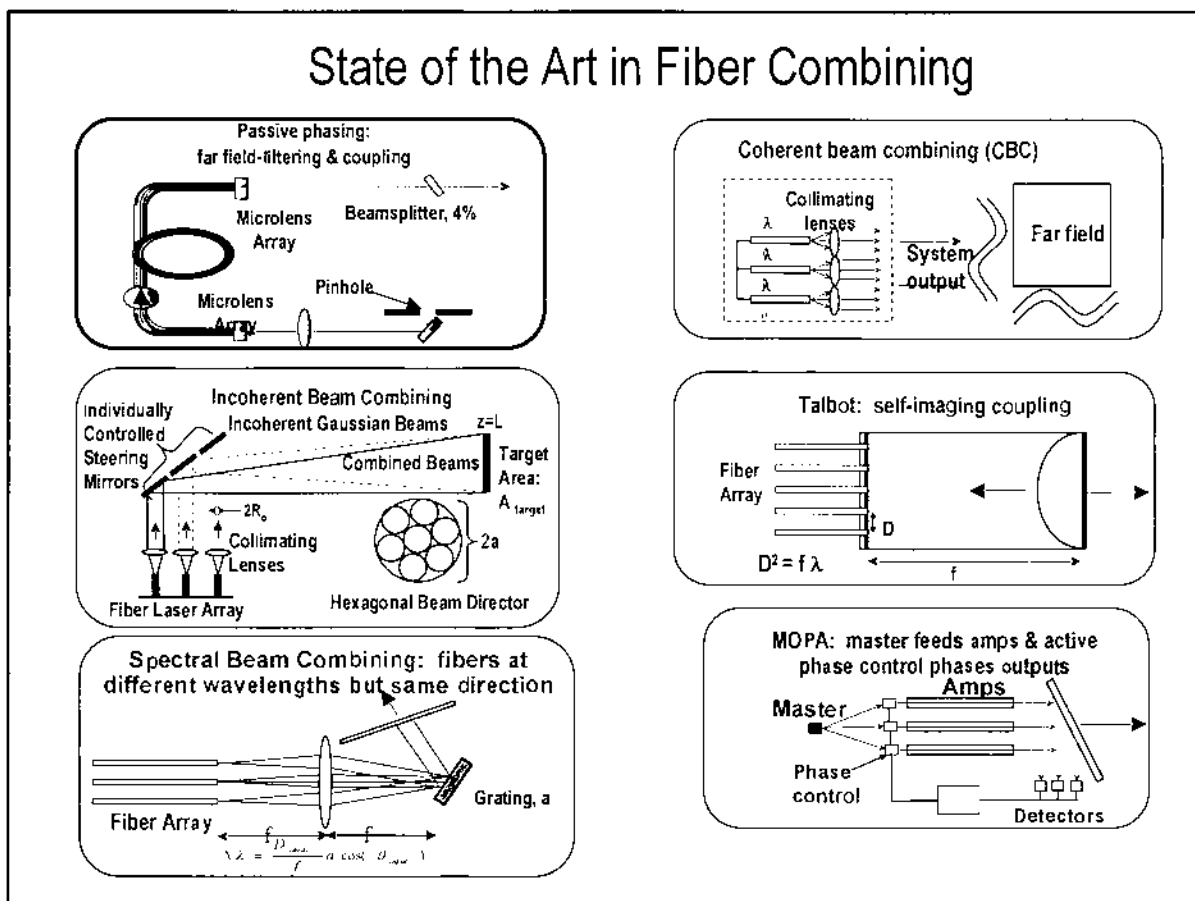

Figure 23. Fiber Laser Beam Combining Techniques (courtesy of the Directed Energy Professional Society).

Typical HPFLs that use fiber optical oscillators or amplifiers as an alternative to bulk rods and slabs have the following technical features [31]:

- Active Gain Medium:
  - Common host glasses and their combinations: Silicates; silicates and phosphates; silicates, phosphates, and fluorides; silicates, germanates, and fluorides; silicates and fluorides.
  - Impurity lasing ions deposited (or doped) in host: Neodymium (Nd^{3+}), Ytterbium (Yb^{3+}), Erbium (Er^{3+}), Thulium (Tm^{3+}), Holmium (Ho^{3+}), Praseodymium (Pr^{3+}).
  - Range of beam wavelengths (λ) produced: 0.48 μm to 2.9 μm.
  - Stretched doped rod into a long thin fiber.
  - Simplifies heat removal (large surface area per unit volume).
- Pump (see Figure 24):
  - Surround lasing fiber with optically transparent jacket.
  - End pump optical jacket with diode lasers.
  - Single diodes or diode bars are coupled into undoped pump fibers
    - Pump fibers are spliced or drawn together with the doped lasing fiber.
    - Pump light is coupled to the outer, undoped outer fiber.
  - Active medium pumped along entire length
    - Pump light then couples into the lasing fiber all along its length.
  - Resonator optics are coupled to the ends of the doped fiber.
- Large Diameter Fibers (see Figure 25):
  - Handle more power.
  - Larger divergence with less beam quality.
  - Longer output fibers before limits are hit.
- Small Diameter Fibers (see Figure 25):
  - Better divergence with greater beam quality.
  - Handle less power before limits:
    - Material limits – melt.
    - Stimulated Brillion Scattering (SBS).
    - Stimulated Raman Scattering (SRS).
  - Shorter output fibers.
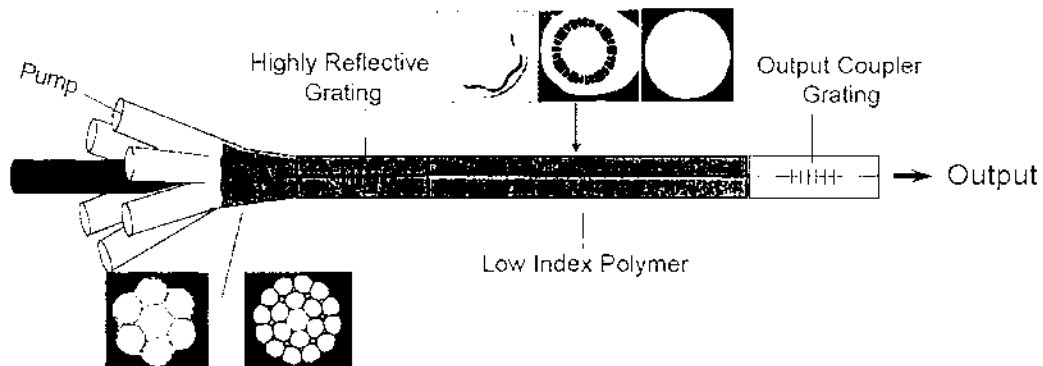
55

Pumping Fiber Lasers

Figure 24. Pumping Fiber Lasers (courtesy of the Directed Energy Professional Society).
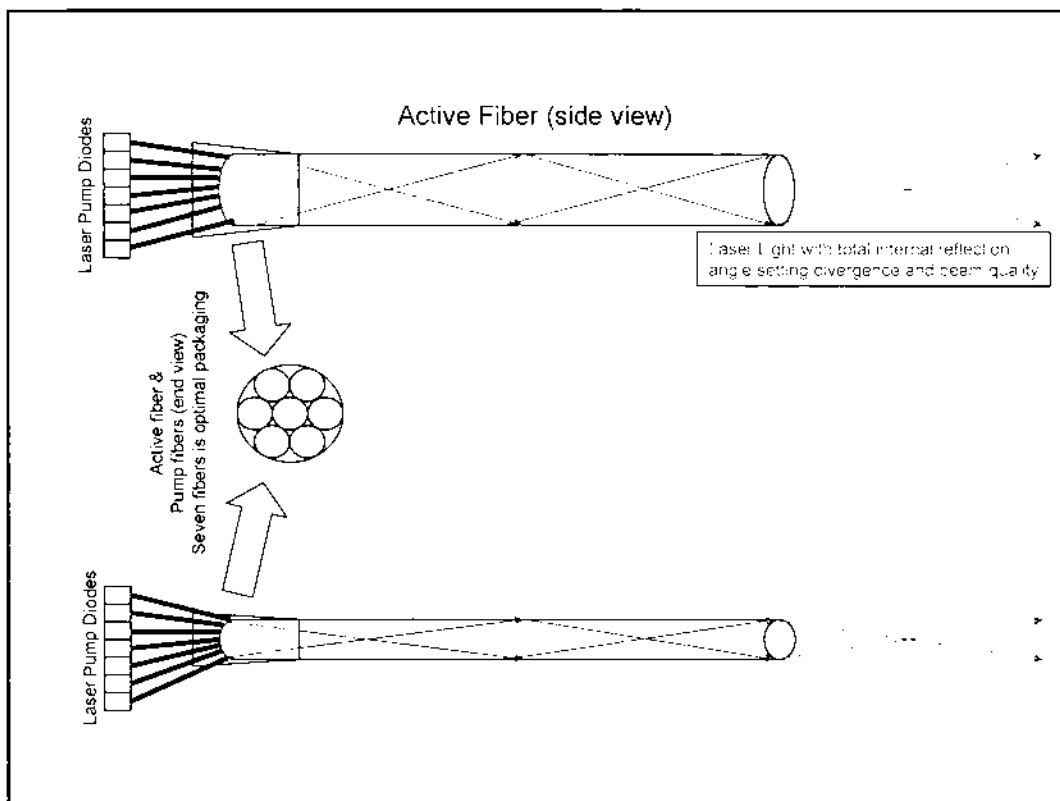

Figure 25. Large and Small Diameter Fiber Lasers (courtesy of the Directed Energy Professional Society).

Figure 26 and Figure 27 show examples of very portable, compact single mode and multimode HPFLs used for industrial applications.
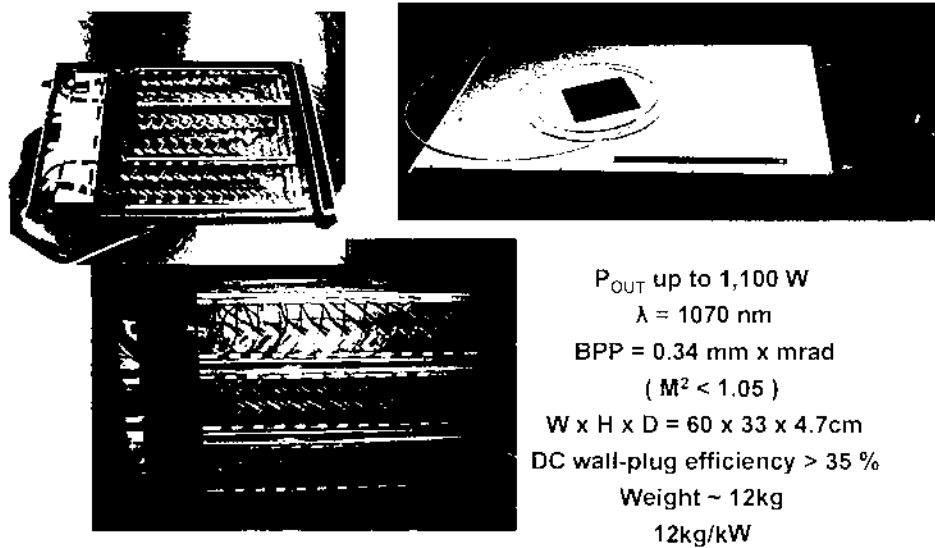
Compact, Lightweight SM Modules

P_{OUT} up to 1,100 W
λ = 1070 nm
BPP = 0.34 mm x mrad
(M^2 < 1.05)
W x H x D = 60 x 33 x 4.7cm
DC wall-plug efficiency > 35 %
Weight ~ 12kg
12kg/kW

Figure 26. Single Mode Fiber Laser Modules (courtesy of IPG Photonics).

Multimode Fiber Lasers

50kW Multimode

- Output beam quality BPP~10 M^2~33
- DC EDE ~ 33%
- Output fiber core diameter 200um
- Dutput NA ~ 0.09
- Output fiber length 15m
- Raman level at full power expected to be ~ -35dB
- Linewidth (FWHM) ~5nm
- Weight ~ 2,500kg
- Size (HxWxD): 1.8m x 2.7m x 0.8m
- Delivered August, 2008
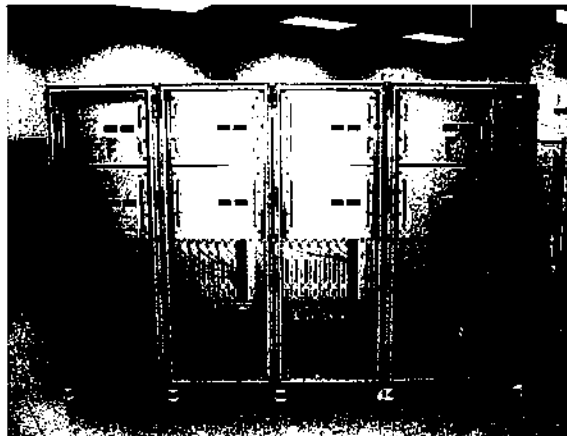
Courtesy of IPG Photonics

Figure 27. Multimode HPFLs.

57

Free Electron Laser

High-energy free electrons from a particle accelerator (e.g., a high-voltage, high-current electron injector gun) can emit amplified, coherent photons when they are sent through an undulator (or "wiggler" magnets), which generates a periodically varying magnetic field with a linear array of permanent or superconducting magnets. The electron accelerator produces a micro-pulse of "electron bunches" moving at relativistic speeds that are laterally accelerated (or "wiggled") by the alternating magnetic fields in the undulator, thus releasing laser photons at optical wavelengths (see Figure 28 to Figure 30). The optical laser radiation is amplified at the double-Doppler-shifted wavelength of the undulator. The resulting laser beam photon energy depends on the electron energy, the undulator period, and (weakly) the magnetic field strength. The electron beam gets spent at the end of the lasing process.
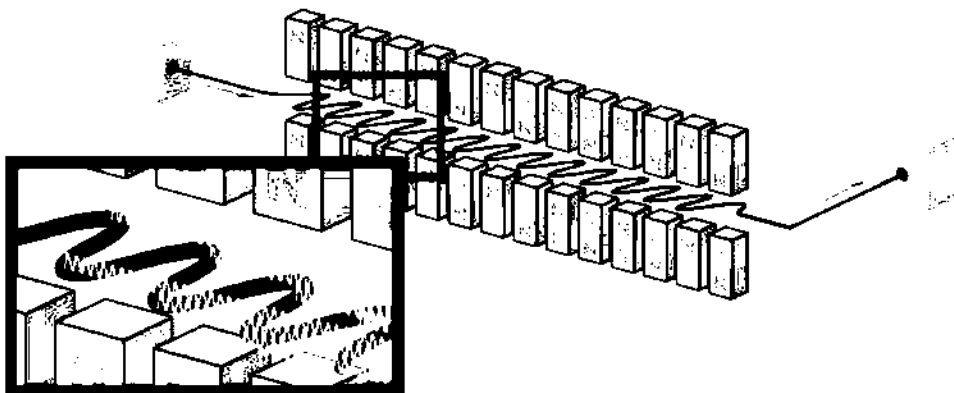

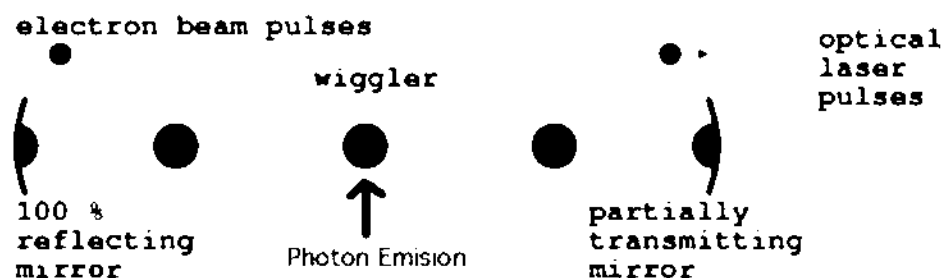**Figure 28. Free-Electron Laser (courtesy of the Naval Post-Graduate School FEL Lab).**

Figure 29. Free-Electron Laser Mechanism (courtesy of the Naval Post-Graduate School FEL Lab).

```
electron beam
                        undulator


resonator                                    mirror
```



```
   .................      ___/\___         ___/\___
                                \\\\\           \\|||\ `
 γ                    γ                  γ
   0    z    λ    0    z    λ    0    z    λ
```

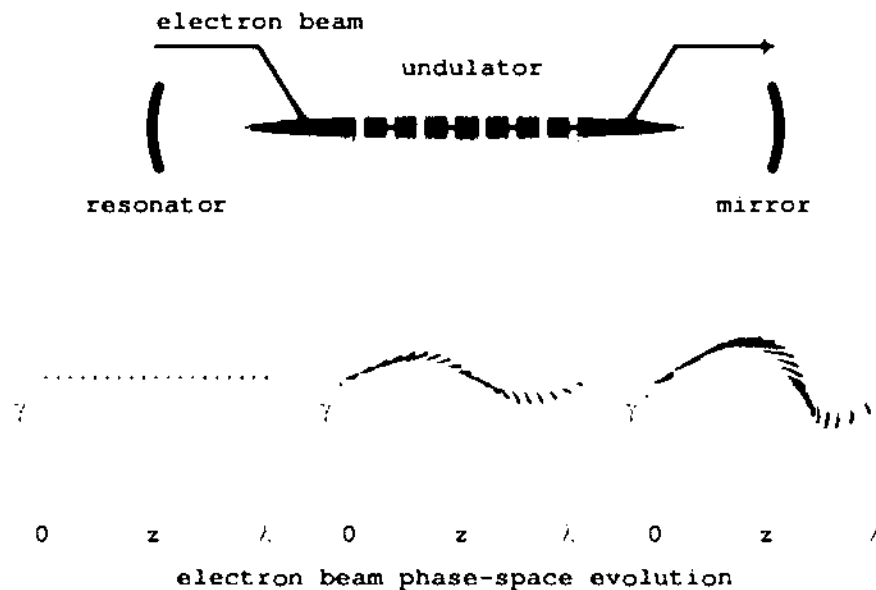electron beam phase-space evolution

Figure 30. Free-Electron Laser Electron Beam Phase-Space Evolution (courtesy of the Naval Post-Graduate School FEL Lab).

In the quantum picture of how FELs operate, the "wiggling" electrons radiate light and that light then gets stored between the resonator mirrors. And additional light radiation (that enters the resonator) in the presence of "stored light" results in stimulated emission, which is the lasing process. The classical interpretation of this process is that the electrons travel with the light radiation and exchange energy with it. Some electrons gain energy while some lose energy to the light radiation. The electrons in the beam will "bunch" within each optical wavelength, thus these bunched electrons will radiate coherently to produce laser light. This mechanism is represented graphically in Figure 29 and Figure 30.

The main appeal of free-electron lasers (FELs) is that they can be built for emission frequencies ranging from the terahertz region, through the infrared and visible spectrum, up to X-rays. Also, a single device often allows wavelength tuning over a large range and the output power can be scaled up very high. As in many spectral regions, it is not easy to make resonator mirrors; many FELs work without such mirrors and rely on amplified spontaneous emission. This can still be relatively efficient if the gain is high enough. One then actually has a superluminescent source. The big disadvantage of FELs is their very large and expensive setup; they can only be used at large facilities. The benefits of FELs are:

- Continuously wavelength tunable, i.e., they can produce different wavelengths *during* operation.
- Designable to produce a range of wavelengths, from microwaves to X-rays.
- Scalable to very high beam power because they use a vacuum for their gain medium – laser medium cannot be damaged.
- Not affected by heat problems that are common in other laser technologies.

- Efficient, generally a FEL can transform 10% (> 60% for microwave tubes) of its energy into laser radiation.
- Reliable, systems now run 24 hours per day for weeks.
- Can produce picosecond laser pulse widths.
- Systems are big (40 m × 60 m) and expensive ($1 Million to $100 Million).

The Naval Sea Systems Command's (NAVSEA) Directed Energy and Electric Weapon Systems (DE&EWS) Program Office is supporting research, development and testing of advanced high-energy/high-power FEL designs for the purpose of deploying them as directed energy weapons onboard warships in the near future. The DE&EWS program is emphasizing the development of disruptive innovations to reduce FEL system size, weight, and operational (and lifetime) cost, as well as to increase overall system operating efficiency. One design that has emerged to reach all of these goals is the recirculating-beam FEL system (RBFEL), which uses a superconducting accelerator, RF power liquid helium refrigerator, an electron beam injector, an electron beam dump, and a modified laser resonator-undulator cavity that boosts the production of amplified, coherent laser photons (see Figure 31). The superconducting accelerator gives good efficiency and gradient while recirculation of the electron beam recovers beam energy to increase efficiency and reduce the beam dump size.
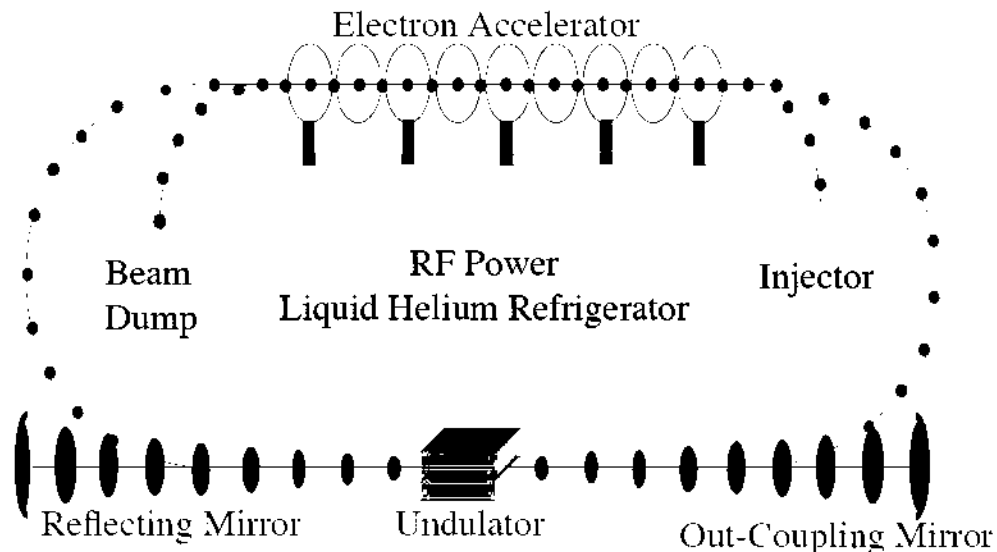

Figure 31. Recirculating-Beam FEL System (courtesy of the Naval Post-Graduate School FEL Lab).

The key (typical) technical features of the Navy RBFEL are as follows:

- Total system volume: 16 m × 4 m × 4 m = 256 m^3.
- Undulator/Wiggler
  - Length: 46 cm to 60 cm.
  - Period: 2.9 cm.
  - Number of periods: 18.
  - Magnetic field strength: 1 Tesla.

- $K \approx 1.5$.[†]
- Electron Beam:
  - Photocathode injector creates picosecond electron pulses at 7 MeV.[‡]
  - Superconducting accelerator increases electron energy to 100 MeV.
  - Peak current: 1100 A.
  - Average current: 0.5 A.
  - Length: 0.1 mm.
  - Radius: 0.1 mm.
  - Electron beam recirculated for energy recovery.
- Optical resonator based on short Rayleigh length optical mode (see Figure 32):
  - Cavity length (resonator mirror separation distance), S: 16 m.
  - Optical waist (natural mode width), w_0: 0.1 mm.
  - Mirror radius of curvature, w: 2.6 cm.
  - Rayleigh length, z_0: 2 cm.
- Optical (Laser Beam) Output:
  - Power: 2 MW.
  - Wavelength, λ: 1 μm (tunable by controlling electron beam, undulator and resonator properties).
- Short Rayleigh length[§] (SRL) optical mode gives several advantages:
  - Reduces optical intensity on resonator mirrors to avoid mirror damage.
  - Single optical wavefront is amplified giving excellent beam quality.
  - FEL interaction is altered with SRL mode.
  - SRL intensifies interaction at mode focus.
    - Rapidly changing optical amplitude and phase.
  - SRL accelerates electron bunching and energy extraction
    - Electrons interact with optical radiation field along undulator.
    - Electrons "see" intense optical electric field at mode focus.
    - Electrons "see" rapidly changing optical radiation phase at mode focus.
- Natural mode width/optical waist (for $S \sim$ meters & laser beam $\lambda \sim$ microns) is millimeters.
- High-power lasers typically run in multiple transverse modes; however:
  - High-power FEL requires short Rayleigh length and small optical waist.
  - High-power FEL amplifies single mode without damage to gain medium (a vacuum).
- FEL efficiency increases as Rayleigh length decreases.
- For megawatt-class FEL system, high operating current plus active mirror alignment system acts to stabilize optical mode against Naval warship vibrations,

---

[†] $K = eB_{rms}\lambda_{und}/2\pi mc^2$, where e is the electron charge, B_{rms} is the root-mean-square magnetic field strength, λ_{und} is the undulator period, m is the electron mass, and c is the speed of light.
[‡] MeV = Mega-electron Volt.
[§] SRL = distance for the area of the beam waist to double.

which usually result in mirror tilts (~ 0 to 400 micro-radians) and drastically reduced beam power, thus maintaining beam power output at maximum design value.
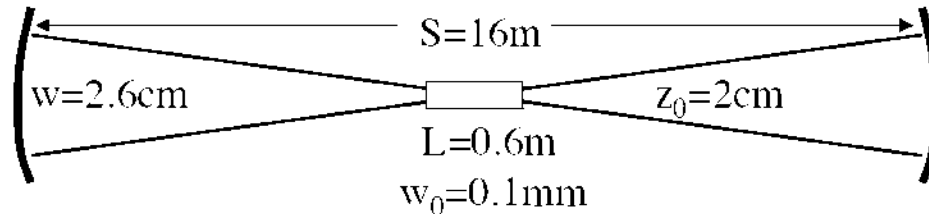

Figure 32. High-Power FEL Optical Resonator (courtesy of the Naval Post-Graduate School FEL Lab).

ESTIMATED PAYLOAD COST FOR LIGHTCRAFT LAUNCH USING A 10 MW BSSSL, HPFL, OR RBFEL SYSTEM

No detailed Lightcraft nano- or pico-satellite payload launch cost estimates can be performed at this time because the high-power solid-state and FEL laser devices are emergent technologies still under development and testing; operational deployment is expected to take place within the next two to five years depending on near-future funding and programmatics. However, Table 1 shows that the average cost to launch a laser-propelled Lightcraft (including payload) to LEO is $3,052 per kg. This figure was based on operations, life-cycle, and maintenance costs plus the cost of using a high-power bulk solid-state laser system that is 50% shared with another user.

The cost estimates shown in Table 1 were compiled in 2003, so this (average) launch cost estimate will likely go down significantly at present (possibly by 20% or more) due to significantly increased system efficiencies realized within each of these emergent advanced laser technologies, reduced system costs due to widespread acceptance, operational deployment along with dual-use commercialization, and system costs that trend downward as technology matures over time, etc. IPG Photonics sells their industrial HPFL systems (e.g., see Figure 27) for prices ranging from $50,000 to $500,000 depending on the beam power (higher beam power = higher price) and system application. Based on these factors, a simple back-of-the-envelope cost estimate for Lightcraft launch of a payload to LEO is approximately $100 to $300 per kg,[**] while the average cost to launch a laser-propelled Lightcraft (including payload) to LEO will be approximately $800 to $2,000 per kg which includes the operations, life-cycle, maintenance, and laser system costs. An in-depth study will be needed to obtain more precise cost estimates for Lightcraft launch using BSSSL, HPFL, and RBFEL systems.

HIGH ENERGY LASER BEAM CONTROL

[**]Costs could be reduced to as low as $20 per kg of payload if Buckytubes are used to construct the Lightcraft.

In order to launch a laser-propelled Lightcraft nanosat or picosat from the ground, sea, or air, it will be necessary to control and steer the high-energy laser (HEL) beam, while at the same time making real-time adjustments to account for platform motion, optical train and atmospheric effects on beam propagation, so that the beam maintains high quality, low-loss, precision contact with the Lightcraft from launch all the way up to LEO. While the atmospheric effects on laser beam propagation were briefly discussed in the Lightcraft Nanosatellite Configuration section of Chapter 2, a more in-depth examination of this phenomenon can be found in Reference 32. In what follows, we briefly discuss what a HEL beam control system is designed to do and what innovations were recently developed by the various DoD directed energy weapons programs that are just now being successfully tested and deployed.

A beam control system is designed to:[††]

- Acquire and precisely track a designated target.
- Handles the HEL beam emitted from the laser:
  - Aligns the HEL beam to the optical train's axis – from the laser resonator to the beam director's exit aperture.
  - Safely relays the HEL beam through the optical train with minimal loss of energy and beam quality.
- Expands the HEL beam and focuses it at the range of the target.
- Places and maintains the HEL beam on the desired target's aimpoint.
- Corrects for beam quality degradations in the optical train or the atmosphere (if needed).

HEL weapons usually have high-power optical trains containing more than a dozen mirrors. However, these systems need to be far more compact with minimal high-power trains. As directed energy weapon applications begin to employ smaller HEL systems, the size, weight and complexity of the accompanying beam control system has come down as well. The typical HEL beam control system includes:[‡‡] 1) a gimbaled beam director, 2) tracking and pointing functions, 3) adaptive optics, 4) acquisition sensors, and 5) target illuminators. Solutions have been recently developed to drive towards a smaller, lighter and simpler beam control system while considering the entire end-to-end system architecture. Existing beam control solutions are robust but large and complex. The technical strides achieved in the past 20 years in wavefront sensing, aperture sharing elements, beam tracking and beam correcting provide new tools to offer a simplified low mirror count beam control system while retaining the ruggedness of function necessary for a laser weapon.

Figure 33 and Figure 34 show schematics of a notional inertially-stabilized pointer/tracker mount and beam control system that was developed by NAVSEA's DE&EWS Program.

[††] D. Kiel, Directed Energy Systems Symposium Short Course, Naval Post-Graduate School, Monterey, CA, 2010.

[‡‡] D. Kiel, Directed Energy Systems Symposium Short Course, Naval Post-Graduate School, Monterey, CA, 2010.

A novel new HEL beam control architecture being tested and deployed by the various directed energy weapons programs that offers reduced complexity and component count, and combines many functions into a compact arrangement has the following key features:[±]

- End-to-end boresight tracker with 0.1 micro-radian root-mean-square accuracy at 10 KHz.
- No beacon illuminator laser (BILL) required.
- Real-time beam quality measurements on target during each engagement.
- Extremely compact and lightweight beam train suitable for ground, airborne and sea platforms.
- Primary mirror which is also a deformable mirror (DM) and a fast steering mirror (FSM).
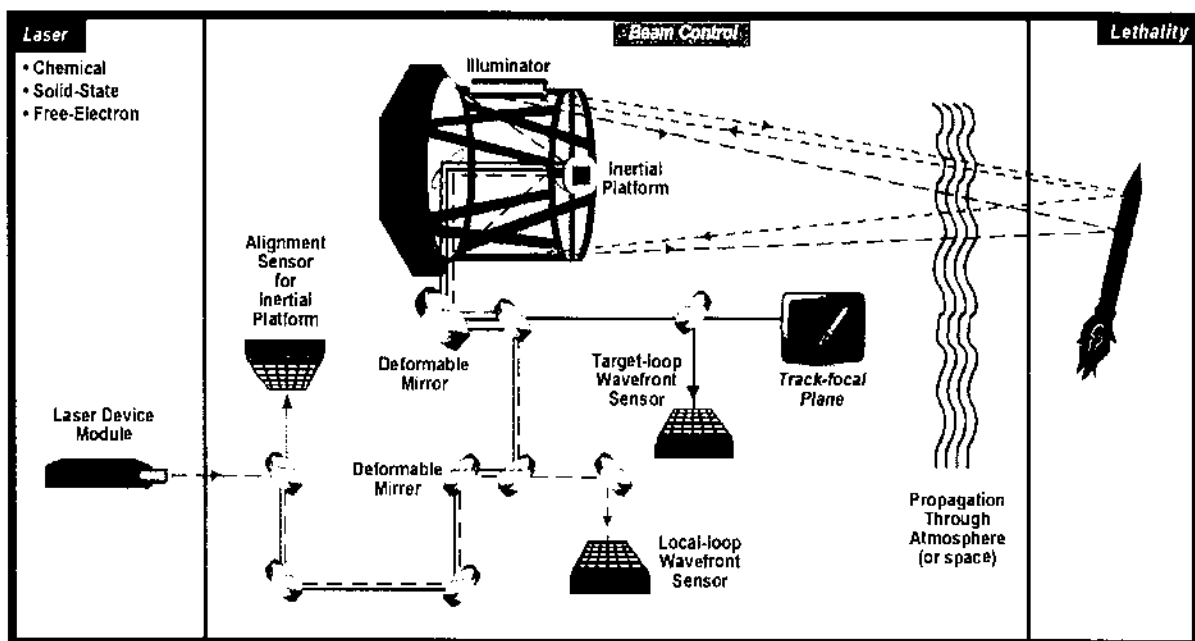

Figure 33. Notional Long Range HEL Beam Control System (courtesy of the Directed Energy Professional Society).
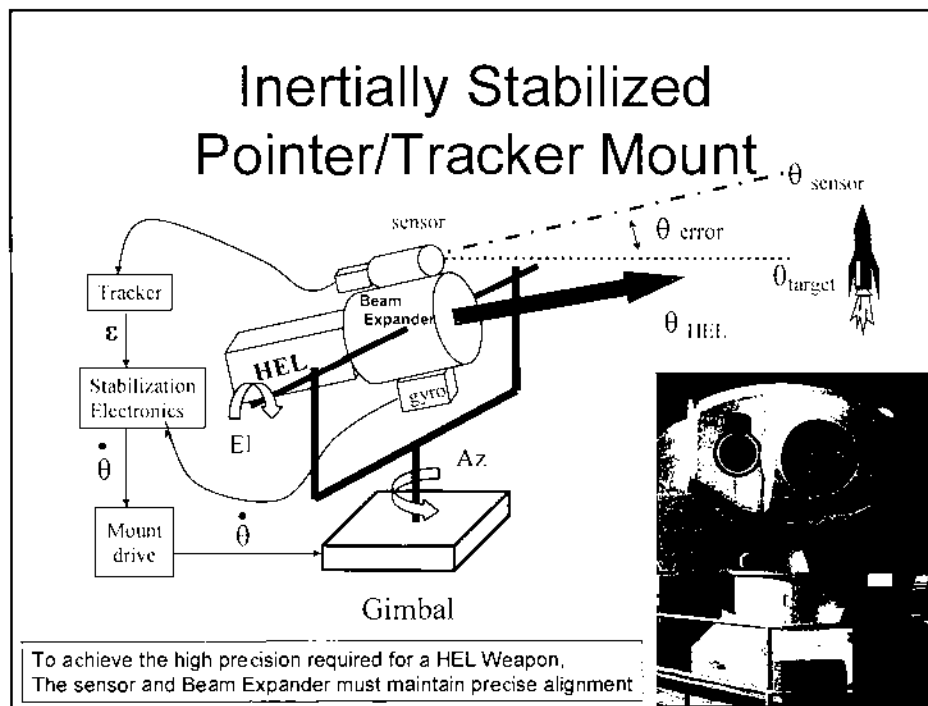
Figure 34. HEL Beam Pointer/Tracker (courtesy of the Directed Energy Professional Society).

In summary, this new architecture has only the HEL module and the beam director. All the measurement and correction functions are integrated into the beam director without increasing the number of high power components usually required in a coude path.[§§] The three major advantages of this architecture are as follows (see Figure 35):[***]

- Minimizing complexity and component count: The optical control architecture has far less than a dozen mirrors plus a turret window and two polarizers between the HEL module and the target. The resulting beam line is considerably simpler, smaller and lighter than current architectures. Almost every component in the beam line performs multiple functions, thereby dramatically reducing the component count. There is only one long-burn DM, one coarse steering mirror (CSM), one FSM, and all of these are integrated into the beam director. This approach also packages all beam control sensors, processors and drivers into the turret assembly.

- End-to-End Boresight and High-Bandwidth Tracking: In this design, the HEL and track illuminating laser (TILL) trackers are integrated onto the same focal plane

---

[§§]Coude is French for "elbow," meaning a beam of light is bent in a zigzag manner through an optical train.
[***]D. Kiel, Directed Energy Systems Symposium Short Course, Naval Post-Graduate School, Monterey, CA, 2010.

and are controlled by a single FSM which is also the primary mirror and DM. This eliminates the traditional split between local and target loop stabilization, combining both into a single controller. This is accomplished so that the high-power path is minimized to its fundamental limit of six mirrors, which are necessary to get the beam from the HEL module through the coude path and out through the exit aperture of the telescope.

- Eliminating the BILL (see Figure 36): The BILL is a solid-state, kilowatt-class laser that measures atmospheric conditions, allowing the beam and fire control systems to compensate for atmospheric turbulence that the HEL beam would encounter in its path to a target. The beam from the BILL bounces off the target and returns to the HEL source, where optical and software equipment measures the amount of distortion in the atmosphere between the HEL source and the target. The HEL adaptive optics system compensates for the distortion using a deformable mirror. Thus, eliminating the BILL was a very important innovation towards decreasing the number of high-power components required in the coude path.
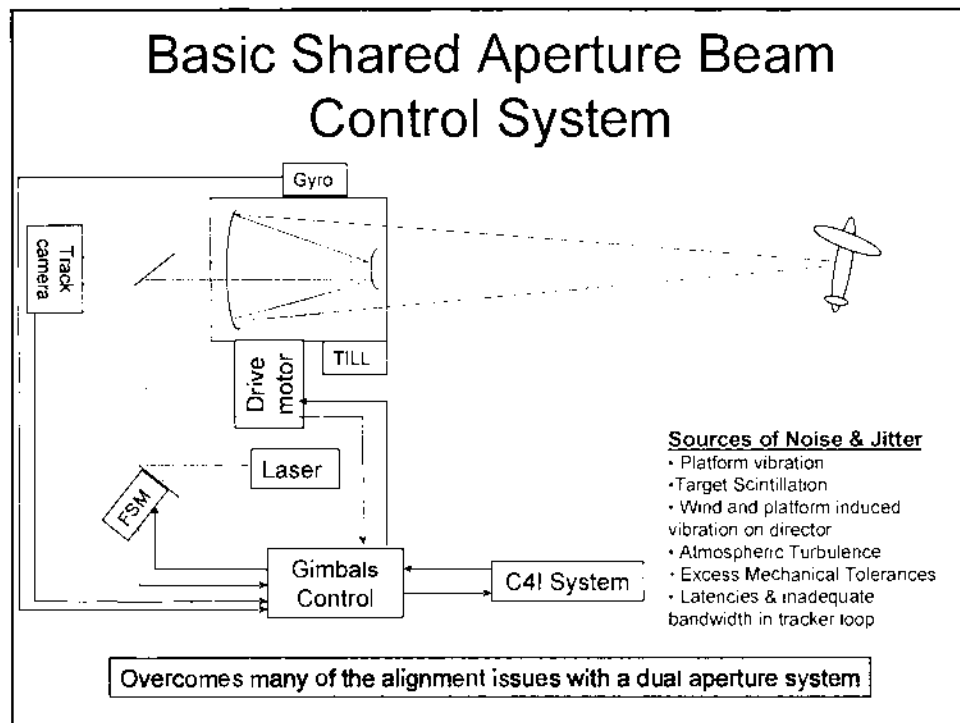

Figure 35. Basic Shared Aperture Beam Control System (TILL = Track Illuminator Laser; C4I = Command, Control, Computing, Communication & Intelligence equipment) (courtesy of the Directed Energy Professional Society).
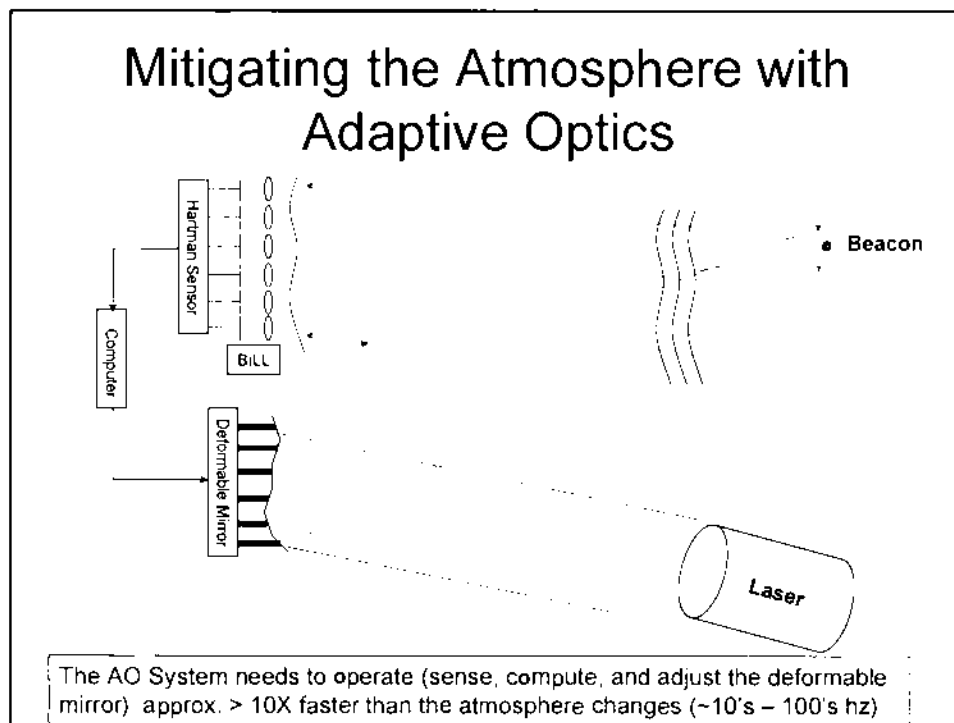
Figure 36. HEL Adaptive Optics System (courtesy of the Directed Energy Professional Society).

All of these HEL beam control innovations can be quickly adapted to laser propulsion applications with little or no additional technical modifications or R&DTE. It is expected that all of the R&DTE work presently being done by the various DoD directed energy weapons/HEL programs can be immediately leveraged for laser Lightcraft nano-/pico-satellite programs should they become established. Primary mirrors with exit apertures of ≤ 10 m will be required to launch laser-propelled Lightcraft from ground/sea to LEO while apertures on aircraft-mounted laser beam control optics will be ≤ 1.0 m.

Chapter 5: Conclusion

To reduce mission costs, advanced technology components and a novel laser propulsion system can make nanosats (and picosats) compact, lightweight, low power, and low cost. By producing a large quantity of nanosats for a given mission, the per-unit cost will be reduced to a small fraction of satellite procurements for traditional missions. Mission operation costs will be minimized by the incorporation of both onboard and ground autonomy, use of heuristic systems, and use of a novel laser propulsion system to launch the nanosats into LEO. Laser propulsion is an enabling technology in which a laser-propelled vehicle, called "Lightcraft," harnesses the energy of a high-energy laser beam and converts it into propulsive thrust.

The laser-propelled Lightcraft is an ETO transportation system that develops quasi-steady (airbreathing) thrust by pulsing at a variable rate along the flight trajectory to orbit, and then when it climbs above the atmosphere it begins to operate in the thermal rocket mode using onboard propellant to convert and expand the laser energy for propulsion. The Lightcraft is spin-stabilized and can be launched vertically upward or on a slant upward trajectory, hover in mid-air, and undergo powered descent and landing. The system is single-stage-to-orbit and completely reusable with no onboard propellant required (the reaction mass is free air), except for the small internal amount of propellant needed for final ascent to orbit and orbital maneuvering. MEMS FEEP thrusters could provide onboard attitude and stationkeeping propulsion. The Lightcraft specific impulse is essentially infinite (several thousand seconds in rocket mode), while payload mass fractions are 50% to 95%.

Laser-propelled Lightcraft systems are simple, reliable, safe, environmentally clean, and could have a very high all azimuth on-demand launch rate. This novel propulsion system reduces space launch costs by two to three orders of magnitude below today's levels, with estimated launch costs of $20 per kg to $600 per kg of payload, not including life-cycle and recurring launch operations costs. The entire Lightcraft launch system is comprised of a ground, sea, or airborne laser beam generator consisting of a power supply, a high-power (megawatt-class) laser beam generator/transmitter using novel beam optics, and automated tracking, hand-off and safety systems.

The most promising military mission for laser-propelled Lightcraft is the placement of Earth and space observing nano-/pico-satellites of up to 3 kg mass into LEO. Such Lightcraft could also serve as a "Lightsat," because it would use the Lightcraft's laser propulsion optics as a telescope for observing military targets on Earth and in space. Such a Lightcraft system appears capable of reaching LEO at 1/5th to 1/10th the cost required for placing a similar Lightsat system into LEO using multistage chemical rocket systems. Other potential missions include using laser-propelled Lightcraft as ground/sea- or airborne-launched kinetic kill weapons to shoot down enemy ballistic missiles. Very innovative near-term missions could also include deploying Lightcraft nano-/pico-satellites to form swarms of small spacecraft which cooperate coherently to form a real distributed system in which the whole is more than the sum of the parts. This would be a constellation of small spacecraft each performing its separate function, but these functions combine to create at a central location a much larger virtual spacecraft, or sensor aperture, that exists solely because of the cooperation of the

spacecraft. This creates coherent RF or optical apertures that are essentially unlimited in size, which could offer unprecedented high-resolution radiometry, hyperspectral imaging, radar, and RF interception (for mapping, surveying, MASINT, SIGNIT), etc.

Launching laser-propelled Lightcraft nano-/pico-satellites to LEO requires megawatt-class lasers. TEXTRON Systems Corporation's proposed 10 MW electron gun-driven CO_2/gas mixture laser is a multi-megawatt-class system that can be implemented now because this technology requires little or no additional R&D. This system offers realistic near-term, low-cost Lightcraft launch capability. However, this system is large, requires a large amount of gas propellant to fuel the laser, and the system infrastructure will cost over $200 million.

The newly emergent bulk slab solid-state, high-power fiber, and free-electron laser technologies being explored by the various DoD directed energy weapons programs offer higher electrical-to-optical efficiencies and overall laser performance, compact and portable system size, less complexity and smaller weight, all at much lower system and infrastructure cost. These lasers are scalable to megawatt-class beam power, and so we roughly estimate that the overall system and infrastructure cost to deploy such laser systems to launch a Lightcraft to LEO will be from several factors to an order of magnitude (or more) lower than for the electron gun-driven CO_2/gas mixture laser system.

Removing the waste heat produced by high-power laser systems is an important factor driving the physical limitations of scaling up the beam output power. An innovative matched-refractive-index liquid is used to rapidly remove the heat produced by a 150 kW bulk slab solid-state laser weapon while the very high surface area-to-volume ratio of high-power fiber lasers allows for the rapid removal of heat from the gain medium without the need for external cooling. Phase-change materials are being explored and devices using such materials have recently demonstrated the ability to store very large quantities of the waste heat produced by high-power solid-state lasers, which is a different way of rapidly removing large amounts of heat from the solid-state gain medium. Unlike solid-state laser systems, free-electron lasers are not affected by heat problems while their gain medium (a vacuum) cannot be damaged.

Launching a laser-propelled Lightcraft nanosat/picosat from the ground, sea, or air into LEO requires controlling and steering the high-energy laser beam, while at the same time making real-time adjustments to account for platform motion, optical train and atmospheric effects on beam propagation, so that the beam maintains high quality, low-loss, precision contact with the Lightcraft during the entire flight. Recent technical innovations in optical train design and other system architecture have evolved beam control devices for high-energy laser weapons toward new implementations. New beam control devices and high-power optical train combinations have a resulting beam line that is considerably simpler, smaller and lighter than current architectures. Almost every component in the beam line performs multiple functions, thereby dramatically reducing the high-power optical component count. This approach also packages all beam control sensors, processors and drivers into a single turret assembly.

In 2005, the AFRL/PRSP (Edwards AFB, CA) concluded their laser Lightcraft propulsion R&DTE program before launching a Lightcraft test vehicle into LEO was demonstrated

69

[33, 34]. At present, AFOSR is funding the Brazilian Air Force's hypersonic shock tunnel study of laser Lightcraft propulsion in collaboration with Leik Myrabo's laser propulsion group at Rensselaer Polytechnic Institute (Troy, NY) [35]. This author recommends that the Department of Defense, in collaboration with NASA, return laser Lightcraft propulsion R&D to the United States and restart the space launch test flight demonstration program of the Air Force X-50LR Lightcraft, which was originally proposed by Dr. Frank Mead [34].

REFERENCES

[1]   Forward, R. L. (1962), "Pluto: Last Stop Before the Stars," *Science Digest* (Aug. issue), pp. 70-75.

[2]   Kantrowitz, A. (1972), "Propulsion to Orbit by Ground-Based Lasers," *Astronautics and Aeronautics*, Vol. 10, pp. 74-76.

[3]   Rom, F. E., and Putre, H. A. (1972), "Laser Propulsion," NASA Technical Memorandum TM X-2510.

[4]   Pirri, A. N., and Weiss, R. F. (1972), "Laser Propulsion," AIAA Paper 72-719, AIAA 5th Fluid and Plasma Dynamics Conference, Boston, MA.

[5]   Harstad, K. G. (1972), "Review of Laser-Solid Interactions and Its Possibilities for Space Propulsion," NASA Technical Memorandum 33-578, NASA Jet Propulsion Lab, Pasadena, CA.

[6]   Pirri, A. N., Monsler, J. J., and Nebolsine, P. E. (1973), "Propulsion by Absorption of Laser Radiation," AIAA Paper 73-624, AIAA 6th Fluid and Plasma Dynamics Conference, Palm Springs, CA.

[7]   Myrabo, L. N. (1982), "A Concept for Light-Powered Flight," AIAA/SAE/ASME 18th Joint Propulsion Conference, Cleveland, OH.

[8]   Myrabo, L. N. (1983), "Advanced Beamed-Energy and Field Propulsion Concepts," BDM/W-83-225-TR, BDM Corp., Final Report for CalTech and NASA-JPL, NASA Contract NAS7-100.

[9]   Myrabo, L. N., and Ing, D. (1985), *The Future of Flight*, Baen Books-Simon and Schuster, New York.

[10] Kare, J. T., ed. (1987), *Proc. of the SDIO/DARPA Workshop on Laser Propulsion*, CONF-860778, Vol. 1 - 3, Lawrence Livermore National Laboratory, CA.

[11] Myrabo, L. N., et. al. (1989), "Lightcraft Technology Demonstrator," Final Technical Report, Contract No. 2073803 for Lawrence Livermore National Laboratory and the SDIO Laser Propulsion Program.

[12] Kare, J. T. (1990), "Ground to Orbit Laser Propulsion Q Advanced Applications," in *Vision-21: Space Travel for the Next Millennium*, edited by G. Landis, NASA Conference Publication 10059.

[13] Kare, J. T. (1990), "Laser Supported Detonation Waves and Pulsed Laser Propulsion," in *Current Topics in Shock Waves*, 17th Int'l Symposium on Shock Waves and Shock Tubes, edited by Y. W. Kim, AIP Conference Proceedings 208, AIP Press, Melville, NY.

[14] Kare, J. T. (1990), "Pulsed Laser Propulsion for Low Cost, High Volume Launch to Orbit," IAF Conference on Space Power, Cleveland, OH.

[15] Lawrence, R. J., et al. (1991), "System Requirements for Low-Earth-Orbit Launch Using Laser Propulsion," in *Proc. of the 6th Int'l Conference on Emerging Nuclear Energy Systems*, SAND 91-1687C, Sandia National Laboratory, NM.

[16] Messitt, D. G., Myrabo, L. N., and Mead, F. B. (2000), "Laser Initiated Blast Wave for Launch Vehicle Propulsion," AIAA-2000-3848, AIAA/ASME/SAE/ASEE 36th Joint Propulsion Conference, Huntsville, AL.

[17] Myrabo, L. N., Messitt, D. G., and Mead, F. B. (1998), "Ground and Flight Tests of a Laser Propelled Vehicle," AIAA-98-1001, AIAA 36th Aerospace Sciences Meeting & Exhibit, Reno, NV.

[18] Mead, F. B., Myrabo, L. N., and Messitt, D. G. (1998), "Flight and Ground Tests of a Laser-Boosted Vehicle," AIAA-98-3735, AIAA/ASME/SAE/ASEE 34th Joint Propulsion Conference and Exhibit, Cleveland, OH.

[19] Wang, T.-S., et al. (2000), "Performance Modeling of an Experimental Laser Propelled Lightcraft," AIAA-2000-2347, 31st AIAA Plasmadynamics and Lasers Conference, Denver, CO.

[20] Wang, T.-S., et al. (2001), "Advanced Performance Modeling of Experimental Laser Lightcrafts," AIAA-2001-0648, 39th AIAA Aerospace Sciences Meeting and Exhibit, Reno, NV.

[21] Wang, T.-S., et al. (2002), "Advanced Performance Modeling of Experimental Laser Lightcraft," *J. Propul. and Power*, Vol. 18, pp. 1129-1138.

[22] Myrabo, L. N. (2001), "World Record Flights of Beam-Riding Rocket Lightcraft: Demonstration of 'Disruptive' Propulsion Technology," AIAA-2001-3798, AIAA/ASME/SAE/ASEE 37th Joint Propulsion Conference, Salt Lake City, UT.

[23] Mead, F. B., Larson, C. W., and Kalliomaa, W. M. (2002), "A Status Report of the X-50LR Program – A Laser Propulsion Program," AIAA/ASME/SAE/ASEE 38th Joint Propulsion Conference, Indianapolis, IN.

[24] Larson, C. W., Mead, F. B., and Kalliomaa, W. M. (2002), "Energy conversion in laser propulsion III," in *Proc. of the 1st Int'l Symposium on Beamed Energy Propulsion*, edited by A. V. Pakhomov, AIP Conference Proc. 664, AIP Press, Melville, NY, pp. 170-181.

[25] Froning, H. D., et al. (2003), "Study to Determine the Effectiveness and Cost of a Laser-Powered 'Lightcraft' Vehicle System – Results to Guide Future Developments," in *Proc. of the 2nd Int'l Symposium on Beamed Energy Propulsion*, edited by K. Komurasaki, AIP Conference Proc. 702, AIP Press, Melville, NY, pp. 242-250.

[26] Froning, H. D., and Davis, E. W. (2006), "Study to Determine the Effectiveness and Cost of a Laser-Propelled 'Lightcraft' Vehicle System," Final Report AFRL-PR-ED-TR-2003-0033, Air Force Research Laboratory, Air Force Materiel Command, Edwards AFB, CA. [See also, Knecht, S. D., and Mead, F. B. (2004), "Increasing Laser Ramjet (LR) Thrust and Coupling Coefficient via Nozzle Design and Prevention of Plasma Wrap-Around," Final Report AFRL-PR-ED-TR-2004-0082, Air Force Research Laboratory, Air Force Materiel Command, Edwards AFB, CA.]

[27] Rumsfeld, D. H., et al. (2001), *Report of the Commission To Assess United States National Security Space Management and Organization*, U.S. Congress and the Dept. of Defense, Washington DC.

[28] Scott, W. B. (2000), *Aviation Week & Space Technology Magazine* article on the 2001 Report of the Commission to Assess United States National Security Space Management and Organization, Nov. 6, 2000, p. 61.

[29] Hasson, V. (2002), "Briefing on Multi-Megawatt Pulsed CO_2 Laser Transmitter for Propulsion Applications," Advanced Concepts Office, AFRL/PRSP, Edwards AFB, CA (Nov. 18, 2002).

[30] Kalisky, Y. (2006), *The Physics and Engineering of Solid State Lasers*, Tutorial Texts in Optical Engineering, Vol. TT71, SPIE Press, Bellingham, WA.

[31] Motes, R. A., and Berdine, R. W. (2009), *Introduction to High-Power Fiber Lasers*, Publ. by the Directed Energy Professional Society, Albuquerque, NM.

[32] Nielsen, P. E. (2009), *Effects of Directed Energy Weapons: High Power Lasers, High Power Microwaves, and Particle Beams*, Publ. by the Directed Energy Professional Society, Albuquerque, NM, Chapter 3.

[33] Mead, F. B. (2007), "Part I – The Lightcraft Technology Demonstration Program," Final Report AFRL-RZ-ED-TR-2007-0078, Air Force Research Laboratory, Air Force Materiel Command, Edwards AFB, CA.

[34] Mead, F. B. (2007), "Part II – Experimental 50-cm Laser Ramjet (X-50LR) Program," Final Report AFRL-RZ-ED-TR-2007-0079, Air Force Research Laboratory, Air Force Materiel Command, Edwards AFB, CA.

[35] Salvador, I. I., et al. (2010), "Experimental Analysis of a 2-D LightCraft in Static and Hypersonic Conditions," *Proc. of the 6th Int'l Symposium on Beamed Energy Propulsion*, edited by C. R. Phipps, AIP Conference Proc., AIP Press, Melville, NY, in press.